SAND2024-08110

Light Water Reactor Sustainability Program

Topical Analyses Related to Co-located Industrial Facilities at Nuclear Power Plants

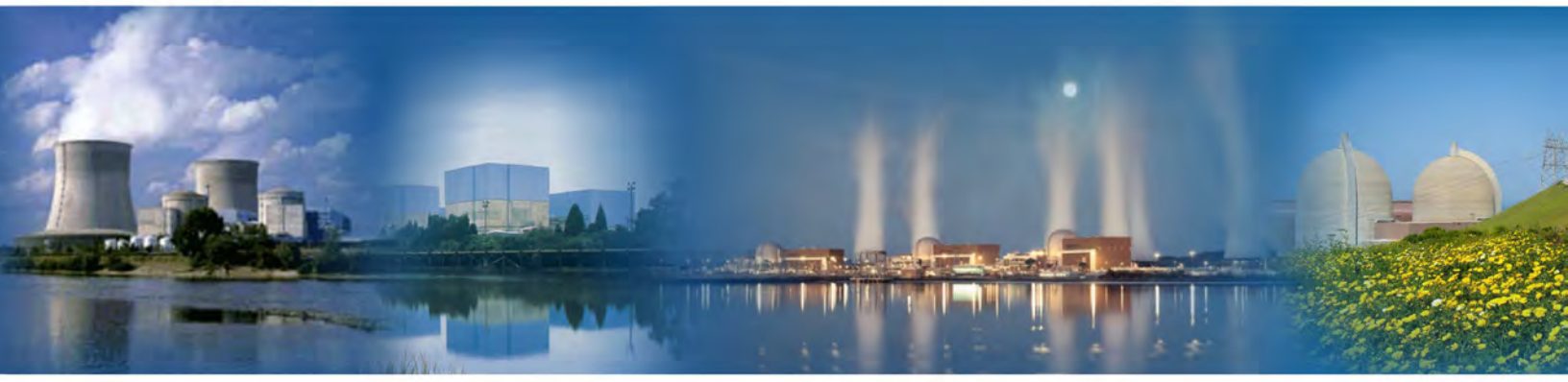

June 2024
U.S. Department of Energy
Office of Nuclear Energy

SANDIA REPORT
SAND2024-08110
Printed June 2024

Sandia National Laboratories

Topical Analyses Related to Co-located Industrial Facilities at Nuclear Power Plants

Melissa S. Louie, Dusty Brooks, and Austin M. Glover

Prepared by
Sandia National Laboratories
Albuquerque, New Mexico
87185 and Livermore,
California 94550

Issued by Sandia National Laboratories, operated for the United States Department of Energy by National Technology & Engineering Solutions of Sandia, LLC.

Available to DOE and DOE contractors from
U.S. Department of Energy
Office of Scientific and Technical Information
P.O. Box 62
Oak Ridge, TN 37831

Telephone: (865) 576-8401
Facsimile: (865) 576-5728
E-Mail: reports@osti.gov
Online ordering: http://www.osti.gov/scitech

Available to the public from
U.S. Department of Commerce
National Technical Information Service
5301 Shawnee Rd
Alexandria, VA 22312

Telephone: (800) 553-6847
Facsimile: (703) 605-6900
E-Mail: orders@ntis.gov
Online order: https://classic.ntis.gov/help/order-methods/

ABSTRACT

This report investigates topics of interest with regard to Nuclear Power Plants (NPPs) utilizing flexible plant operations and generation (FPOG). Previous reports have identified the risk associated with co-located hydrogen generation facilities. This report evaluates special topics with regard to co-location of both hydrogen and syngas production facilities. A literature review was conducted to evaluate overpressure mitigation techniques that may be available to the NPP to reduce the consequence of an overpressure event. Also, the overpressure consequence of a catastrophic hydrogen storage tank failure event was analyzed. A comparison of the similarities and differences between the methodology utilized in HyRAM+ and Regulatory Guide 1.91 (R.G. 1.91) was performed for overpressure analysis. Also, the trinitrotoluene (TNT) equivalency methodology was utilized to evaluate an overpressure event at a Syngas production facility.

CONTENTS

LIST OF FIGURES

LIST OF TABLES

ACRONYMS AND TERMS

Acronym/Term	Definition
AFRP	aramid fiber reinforced plastic
BST	Baker-Strehlow-Tang
CFRP	carbon fiber reinforced plastic
DDT	deflagration to detonation transition
FPOG	flexible plant operations and generation
GFRP	glass fiber reinforced plastic
HyRAM+	Hydrogen Plus Other Alternative Fuels Risk Assessment Models
LNG	liquid natural gas
MCA	maximum credible accident
NPP	nuclear power plant
PPE	personal protective equipment
PTSD	post-traumatic stress disorder
R.G.	Regulatory Guide
Syngas	synthetic gas
TBI	traumatic brain injury
TNT	trinitrotoluene

1. INTRODUCTION

There are several topics of interest for Nuclear Power Plants (NPPs) to weigh when considering utilizing flexible plant operations and generation (FPOG). Hydrogen and synthetic gas (syngas) generation facilities are two options for plants when considering FPOG. Facilities that generate, store, or otherwise contain hydrogen or syngas may be at risk for overpressure events that can potentially be harmful to people as well as infrastructure in the vicinity. For example, an accidental release of hydrogen from the system can ignite into a vapor cloud explosion. Operational errors or system failures may also lead to overpressure within hydrogen-containing vessels and cause a pressure vessel burst. The overpressure and impulse from an explosion can both contribute to the harm experienced by a person or building. A review of relevant literature reveals that there are several potential methods under consideration for use in overpressure mitigation, some of which are already used commercially in a variety of industries. These methods can be used to reduce harm to people and the built environment. They are presented in terms of three overarching categories: explosion isolation, explosion and flame front suppression, and attenuation of overpressure and impulse through energy redirection. Also, this report evaluates the methodology utilized in Hydrogen Plus Other Alternative Fuels Risk Assessment Models (HyRAM+) and that prescribed in Regulatory Guide 1.91 (R.G. 1.91). And two additional overpressure consequence scenarios were evaluated: a catastrophic tank failure containing hydrogen and a vapor cloud explosion at a syngas production facility. The results of these calculations can inform risk evaluations.

2. OVERPRESSURE MITIGATION LITERATURE REVIEW

The methods for mitigating the effects of a blast from a hydrogen plant were categorized into three groups by mechanism: blast isolation, blast suppression, and overpressure attenuation. The blast isolating techniques are meant to protect equipment within the system that is not directly involved in the explosion, by isolating the area affected by the blast. The suppression techniques are methods of slowing or quenching a flame front and preventing further combustion or propagation. The overpressure attenuation techniques are ways to reduce the amount of overpressure, and in some cases, impulse, experienced by a person or building in the vicinity of the blast. Within each category, blast mitigation techniques may be reactive to the accumulation of gas or to an explosion, or passive and always present in the facility.

2.1. Blast Isolation

The isolation techniques reviewed are all triggered when an explosion is detected, and their purpose is to protect equipment not directly involved with the initial explosion from secondary explosions. One method is mechanical; active valves can close when an explosion is detected elsewhere in the system, or passive valves can close in reaction to a certain overpressure. Active valve solutions have already been commercialized by companies such as IEP Technologies [1] and ATEX Explosion Protection [2]. Passive valves are also available commercially through companies that include IEP Technologies, ATEX Explosion Protection, and Boss Products LLC [3].

Figure 2-1. Depiction of mechanical isolation using a high-speed valve [1].

Chemical suppression techniques can also be used as an isolation method. For example, IEP Technologies offers a solution wherein a chemical suppressant can be discharged into piping or duct work to slow and prevent propagation of an explosion flame front through the piping system.

These isolation techniques are meant to protect equipment connected to a vessel in which an explosion has occurred; in other words, they are retroactive responses to an explosion. For a hydrogen facility, an explosion within a storage vessel is unlikely because no oxygen would be present within the piping network. In the event of a leak, the high-pressure hydrogen would be discharged from the system into the air and any potential explosion would happen outside of the vessel instead of inside it. However, it is possible that even an explosion external to the piping could cause a flame to propagate within the piping as well, in which case this mitigation method could still be somewhat helpful for internal protection of other equipment within the system.

2.2. Blast Suppression

The blast suppression techniques reviewed in this report are somewhat similar to the chemical isolation method in that they are used to either prevent ignition when an explosion is imminent or to quench and slow the flame front once combustion occurs. In comparison to the isolation methods described previously, the suppression techniques in this section are broader in application and can be used in a larger space than just within a piping network.

Multiple suppressants can be used for this purpose. Several studies investigate the use of water mists from sprinkler systems for blast mitigation via experiments or computational analysis. In these studies, a water mist was deployed in the area of the explosion. There is some agreement and some discrepancy regarding the mechanisms for blast reduction. Grujicic et. al. describes two hypothesized mechanisms as momentum transfer into the aerosolization of larger water droplets, and the dissipation of blast energy as heat used to evaporate smaller water droplets [4]. The evaporation mechanism is also referred to as quenching by van Wingerden [5]. Quenching also prevents secondary combustion reactions and propagation of the flame front because the water vapor can help dilute the fuel-air mixture to below the flammable limit [5].

Grujicic et. al. and van Wingerden attribute blast mitigation via water mist to both mechanisms. However, Schwer and Kailasanath [6] ascribe the majority of blast mitigation to momentum extraction and claim that the vaporization effects are small because the shock wave "temperature is not extreme and the time is very short," and because the vaporized water contributes to gas density and increases the gas pressure, which "partially [cancels] out the effect of lowering the pressure through lower gas temperatures." Schunk et. al. [7], meanwhile, conclude that fire extinguishment and quenching is the main contributing mechanism because of their observation of water droplet acceleration and break-up occurring in the airstream downstream of the shock wave after the shock wave had already passed through. The variability in the experiments may be one reason for the divergent conclusions on the blast mitigation mechanism. One such example is the type of explosive used for the experiment; Schunk et. al. used Combination B to generate an explosion while van Wingerden used petrochemical gas and Schwer and Kailasanath used trinitrotoluene (TNT). The fuel used for the explosion may affect the properties of the shock wave and the mechanism for blast mitigation.

In terms of effective location of the water mist system, Schunk et. al. found that the explosion should occur within the misted area in order for the overpressure and impulse to be meaningfully reduced [7]. Schwer and Kailasanath found that the overpressure mitigation of this method is more effective farther from the point of deflagration or detonation.

Several of the papers concur that water deluge can reduce blast overpressure and prevent flame propagation in appropriate situations, but it can also increase overpressure or cause further issues if not used properly. For example, the water spray may introduce more turbulence into the gas mixture, which would increase the propagation speed of the flame front and the Mach flame speed of any secondary reactions that might occur, causing an increase in overpressure [5], [6]. The water may also provide an ignition source for the leaking gas, either through sparking with electrical equipment or through electrostatic charging of ungrounded objects in the system [5]. Van Wingerden found that the water spray was found to work more effectively in a congested environment and actually made the overpressure effects worse with a more open, low-congestion system design because the turbulence effects dominated any momentum transfer or quenching effects that the water might have had on the flame front [5].

The water deluge mitigation method may potentially be useful at a hydrogen plant. If any part of the system is located indoors, if, for example, there is any small-scale storage or generation at the facility, it could be simple to integrate the water spray system similar to the existing sprinkler system. Depending on the installed sprinkler system and relevant regulations, the sprinkler system itself can be used for blast mitigation. If permitted by the governing codes and standards, sprinkler nozzles discharging very small (less than 10 micron) or very large (greater than 200 micron) droplets would most effectively mitigate blast effects; the small droplets can evaporate in a flame while the large droplets provide objects on which the flame can impart momentum [5]. Proper classification, use, and grounding of electrical equipment can help prevent the water deluge from causing ignition of the accumulated gas.

It may be less straight-forward to use a water mist or spray for blast mitigation in larger-scale, outdoor hydrogen facilities. For example, storage equipment that is located outside and does not have any sort of roof or enclosure would require an additional structure on which to mount the water sprinkler system. This required infrastructure would introduce extra costs and could act as an obstruction to any leaking hydrogen. Obstructions are undesirable because they can increase turbulence in the leaking fluid flow, which could accelerate a flame front and worsen the effects of an explosion if one occurs. Additionally, an outdoor environment is generally open and has little congestion to start with compared to an indoor environment. The open and low-congestion conditions are not well suited for the water deluge mitigation method, as previously discussed. In addition, van Wingerden suggests that the water deluge must be deployed in the area before the explosion occurs, in other words, before delayed ignition. For hydrogen, the probability of immediate ignition (resulting in a jet fire) is higher than the probability of delayed ignition (resulting in an explosion), but the consequences may be lower and more localized. Thus, deploying a water mist on a hydrogen leak that may have already ignited into a jet fire may extinguish the flame and increase the probability of the higher-consequence delayed ignition event instead.

If done properly, though, using a water mist on an area of leaking but unignited hydrogen could prevent ignition through inerting of the hydrogen-air mixture. Jones et. al. performed water mist experiments on hydrogen-air explosions and found that a mist that has a sufficient volume density in the hydrogen-air mixture can increase the lower flammability limit hydrogen concentration, which is usually around 4% by volume. The droplet size as well as the mist volume density matter greatly for inerting to work. The work by Jones et. al. shows that a water mist can be used to prevent a blast, not just to mitigate the effects of a blast that has already occurred [8].

The reviewed literature may be a helpful starting point for pointing towards a water deluge as a blast mitigation method depending on the system design and configuration. However, there are differences between many of the reviewed papers and a hydrogen plant that may mean the conclusions do not translate exactly to hydrogen systems. As mentioned previously, most of the reviewed papers used hydrogen as the fuel for the explosion; different explosives may behave differently depending on their combustion properties. Additionally, many of the experiments were conducted in environments in which blast and mitigation behavior may be different than in a hydrogen plant. For example, Schunk et. al. performed experiments in both a 4.35 m x 2 m x 2.8 m tunnel and in a 400 mm-diameter shock tube, van Wingerden cites full-scale experiments done in a 28 m x 12 m x 8 m tunnel, and Schwer and Kailasanath's computational work used simulations to model explosions in confined spaces. Even though the experiments by Jones et. al. were done with a hydrogen-air mixture, the test setup was in a 760 mm x 560 mm x 280 mm explosion cabinet, which is a confined space and at a much smaller scale than a hydrogen plant. The scale and setup of each experiment may have an impact on the shock wave and mitigation behavior. In addition, detonations

were realized in many of the experiments (although Jones et. al. did characterize their explosions as deflagrations). Ehrhart et. al. considers unconfined hydrogen flame speeds to generally be around Mach 0.35 [9], which can cause a deflagration but not a detonation. Even shock wave reflections from any obstacles or surfaces in the area would be unlikely to accelerate the flame into a deflagration to detonation transition (DDT) [10]. The potential difference in the reaction of a deflagration or detonation to a water deluge is also a consideration when determining whether this method would be practical for a hydrogen plant.

Substances other than water, such as two-phase chemicals and powders, have also been studied as explosion suppressants. Del Prete et al. found that aqueous foams, which are "cellular two-phase system[s] in which gas cells are enclosed by thin liquid films," can be used to reduce the peak overpressure from an explosion [11]. This conclusion was determined based on an experiment in which a detonation device in a plastic tent was covered in an aqueous foam formulation and set off. A schematic for this experiment is shown in Figure 2-2.

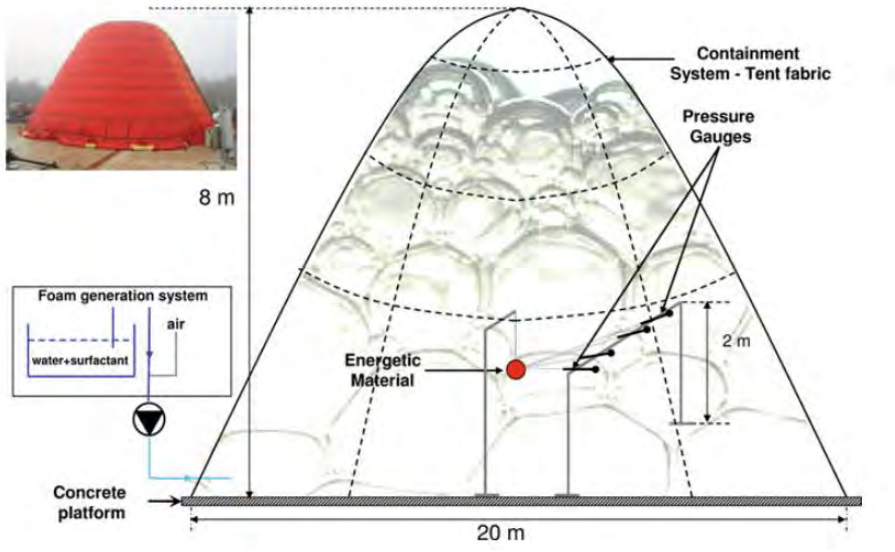

Figure 2-2. Experimental setup showing dry aqueous foam explosion suppression method [11].

Commercial chemical suppressants for explosion control exist. ATEX and CV Technology both offer dry powders that can be discharged into a vessel if an explosion is detected within it [12], [13]. Pontalier et. al. investigated solid suppressants in the form of other solid and granular materials such as sand, glass, steel, ceramic, porcelain, plastic, claydite, polyethylene, perlite, and pumice [14]. Experiments in which an explosive was detonated within a bulb filled with a granular material revealed that the presence of the chemical suppressant did lead to overpressure mitigation, "mainly due to the transfer of heat and momentum" [14]. An image of this experimental setup is shown in Figure 2-3.

Figure 2-3. Experimental setup showing detonable explosive inside a glass bulb packed with iron powder [14].

The setup in Figure 2-3 shows how the explosion occurs at a point within the solid powder, which is not directly applicable to a leaking hydrogen facility since the delayed ignition point and overpressure origin can occur at any location. In addition, the hydrogen leak is in the open air and not contained within a confined space in which a solid granular material can be packed. Nevertheless, the results of this paper are still helpful in showing that the presence of granular materials around a blast region may assist with blast mitigation. For example, the reflection of the blast wave against the ground may be reduced if there is sand or another granular material present on the ground, but this proposed configuration is different from that presented in [14] and would require more study to understand its efficacy.

Aqueous chemicals and dry powders, while potentially effective for blast mitigation, may be challenging to implement in a hydrogen plant. The aforementioned examples all show that, for mitigation to be most effective, the explosive region should be completely covered or submerged in the suppressant. The previous paragraph explains why submerging the explosive region is not possible: a hydrogen leak would not be contained, and its location is unpredictable. Possibly, the chemical suppressant or powder could be sprayed over an area in a hydrogen facility when an explosion is imminent. However, this method would not exactly mirror the tested methods, and could potentially increase the consequences of the explosion through increased turbulence and mixing of hydrogen and air. Furthermore, non-water suppressants may be more expensive, difficult to clean, and could negatively impact the environment or people in the area; granular materials especially could harm people in the vicinity if they are accelerated away from an overpressure origin. Water, therefore, seems a more appropriate choice than aqueous foams or dry powders for blast suppression in a hydrogen plant, as long as the system design is evaluated and determined to be appropriate for blast mitigation via water deluge.

2.3. Redirection of Blast Wave Energy

Harm and damage can occur to people and infrastructure from the magnitude and short duration of energy transfer from the shock wave from an overpressure event. In the reviewed literature, attenuation of overpressure and impulse for a vulnerable person or building is achieved through redirection of this energy away from them, using barriers such as blast walls. The main mechanisms for energy redirection are reflection, absorption, and diffraction; these mechanisms help minimize

the amount of energy transmitted through the barrier and to the people and building that it is meant to protect. While some of the cited literature in this section was based on work done specifically on hydrogen-air explosions, there are not as many as for other explosions.

2.3.1. Traditional Blast Barriers

Solid blast barriers are currently already used in industries adjacent to hydrogen, such as oil and gas storage and pipelines, liquid natural gas (LNG) infrastructure, and chemical plants [15]. There is limited available information on the usage of blast barriers in existing hydrogen plants. However, research on hydrogen-air blast mitigation exists and NFPA 2, a hydrogen-specific code, provides some discussion of how blast walls can be used to protect equipment and structures [16]. Blast barriers can be freestanding or incorporated into existing infrastructure onsite.

Unlike the suppression methods in the previous section, walls not only attenuate overpressure, but also provide protection against projectiles that are propelled by the blast wave. This extra layer of protection is not trivial. Overpressure values published by LaChance et. al. show that indirect overpressure harm such as skin lacerations and fatalities from missile wounds occur at lower overpressures than direct harm such as eardrum rupture, lung hemorrhage, and immediate blast fatalities [17].

Currently, the two main materials used for blast walls are concrete and steel. Modular blast walls made of both materials are popular in the industry because they can be reconfigured and relocated easily, rather than being permanent, immovable fixtures. Since it is unlikely that an already-built hydrogen plant would be reconfigured and the locations at risk of explosions would change, the mobility of blast walls may not be as important as other more dynamic applications, but it is still an aspect that can be considered.

a)  b) 

Figure 2-4. a) Block Moulds modular concrete blast wall [18] and b) BDI prefabricated steel blast wall (cropped from [15]).

Redguard argues that steel is more desirable than concrete as a blast wall material because concrete is susceptible to weakening due to condensation [19]. Condensation could potentially be a constant presence at a facility like a hydrogen plant, where water vapor is constantly being produced at vent stacks and any other locations where hydrogen encounters oxygen in the air. Its malleability also helps it absorb some of the blast energy [19], compared to concrete, which is more brittle and has been observed cracking under a blast wave when overcome by tensile stress [20]. The high strength of steel also allows it to be constructed thinner and lighter, which makes construction and moving of the blast walls easier even when comparing modular structures of both materials. These points indicate that steel may be a preferable blast wall medium than concrete for hydrogen facilities, but

other features like cost and material availability also factor into the blast wall material choice. Nonetheless, both materials have proven to be effective for reduction of overpressure harm inflicted on vulnerable people and buildings.

Modifications can be made to the basic blast wall materials to improve their lifetime and performance. Kim et. al. found that increasing the wall thickness of concrete barriers reduces the structural damage they sustain [21]. Concrete barriers can also be strengthened through reinforcement with steel, which has been experimentally found to reduce the displacement of the wall during the blast and reduce the amount of cracking in the structure, leading to an improved blast capacity [21].

The geometry of the blast barrier and its distance from the overpressure origin can affect its overpressure attenuation capabilities and the damage it sustains. Experiments by Liu et. al. on the effects of hydrogen-air explosions on a protective wall compared overpressure profiles over space when the wall height and distance from the explosion was varied [22]. Since the reflection of a shock wave against a wall can actually increase overpressure, taller walls translate to larger surfaces for shock reflection, and increased peak overpressures in the area containing the explosion. A taller wall can therefore provide more protection outside of the blast wall but increase the harm to people and equipment upstream of the wall. A tall barrier wall in conjunction with leak monitoring or detection systems can be one way to ensure that all people evacuate the area upstream of the wall before a blast occurs if an explosion is imminent. In terms of the distance between an explosion and the barrier wall, Liu et. al. found that a smaller distance led to a region of heightened overpressure and temperature that was more dangerous to people upstream of the wall than if the explosion-to-wall distance were larger [22]. In terms of protected people downstream of the wall, Sochet et. al. found that barrier walls located closer to an overpressure origin provide better attenuation of the blast wave downstream of the wall [23]. In any case, the distance between an explosion and the blast wall cannot be predicted in a hydrogen facility since a leak could happen from any component that contains hydrogen. Nevertheless, this paper provides evidence that, while varying the wall height and distance from the explosion point has some effect on the overpressures experienced within the wall, any wall height and placement will provide overpressure attenuation downstream of the wall. This finding reinforces the importance of ensuring that, when an explosion is inevitable, the at-risk area is detected so people can relocate to the safe areas of the facility.

Traditional blast barriers are a well-established method of overpressure mitigation in many industries. They have been proven to protect people and infrastructure from harm due to overpressure and accelerated debris from the blast.

2.3.2. Alternative Blast Barrier Geometries

2.3.2.1. Solid Barriers

There is ample literature available on blast barriers with modified geometries. Sochet et. al. also compared the efficacy of different wall cross-sectional shapes in blast mitigation [23]. They explain that, when a barrier is present during an explosion, the blast wave reflects off the barrier and collides and combines with the incident blast wave to create a Mach stem. There is a relaxation of this Mach stem that occurs at the top of the wall. Sochet et. al. asserts that a sufficiently tall and thick parallelepiped is theoretically the most effective cross-sectional shape, because its angles allow for substantial relaxation of the Mach stem and overpressure. Since a barrier of this shape would be

quite large, it would require a significant amount of space, construction materials, and money. However, the paper also provides general guidance for blast wall design based on experiments done with walls with trapezoidal cross-sectional shapes with different angles and orientations.

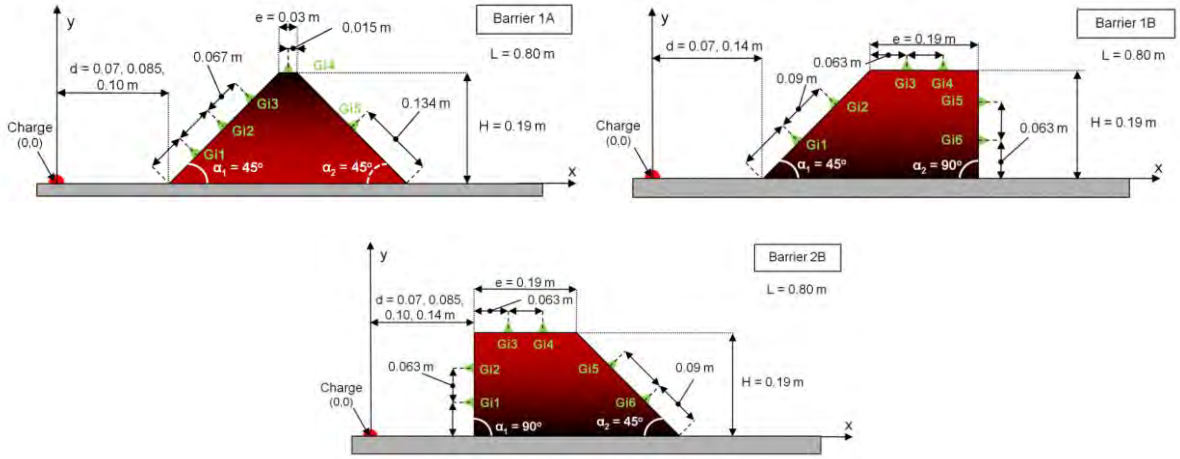

Figure 2-5. Example geometries for walls with trapezoidal cross-sections [23].

The experiments by Sochet et. al. revealed that the three main geometrical parameters of interest are wall height, thickness, inclination angles of the front and rear faces (α_1 and α_2 in Figure 2-5), and the barrier position in relation to the overpressure origin. They suggest that, given space and financial constraints, the height and thickness of the wall should be maximized so the surface area of the wall that the shock wave will encounter will be maximal. The angle of inclination of the upstream face of the wall affects both the overpressure attenuation ability of the wall and the load sustained by the wall itself. For a blast wall located close to the overpressure origin, a 90° inclination for angle α_1 provides a large overpressure screening effect for downstream targets but also causes the front wall face to experience a high overpressure load. Nevertheless, 90° angles for either or both angles of inclination (on the front and back faces of the wall) provide the most space-efficient geometry and would likely therefore remain the preferred geometry to smaller inclination angles for many facilities.

Nozu et. al. also tested the overpressure mitigation capabilities of walls with different cross sections [20]. They found that energy dissipation through diffraction against the top edge of the wall allowed the walls with Y- and T-shaped cross-sections to mitigate the blast pressure more effectively because the diffraction happened twice. Figure 2-6 shows pressure contours for these two geometries compared to the traditional barrier wall geometry with an I-shaped cross-section.

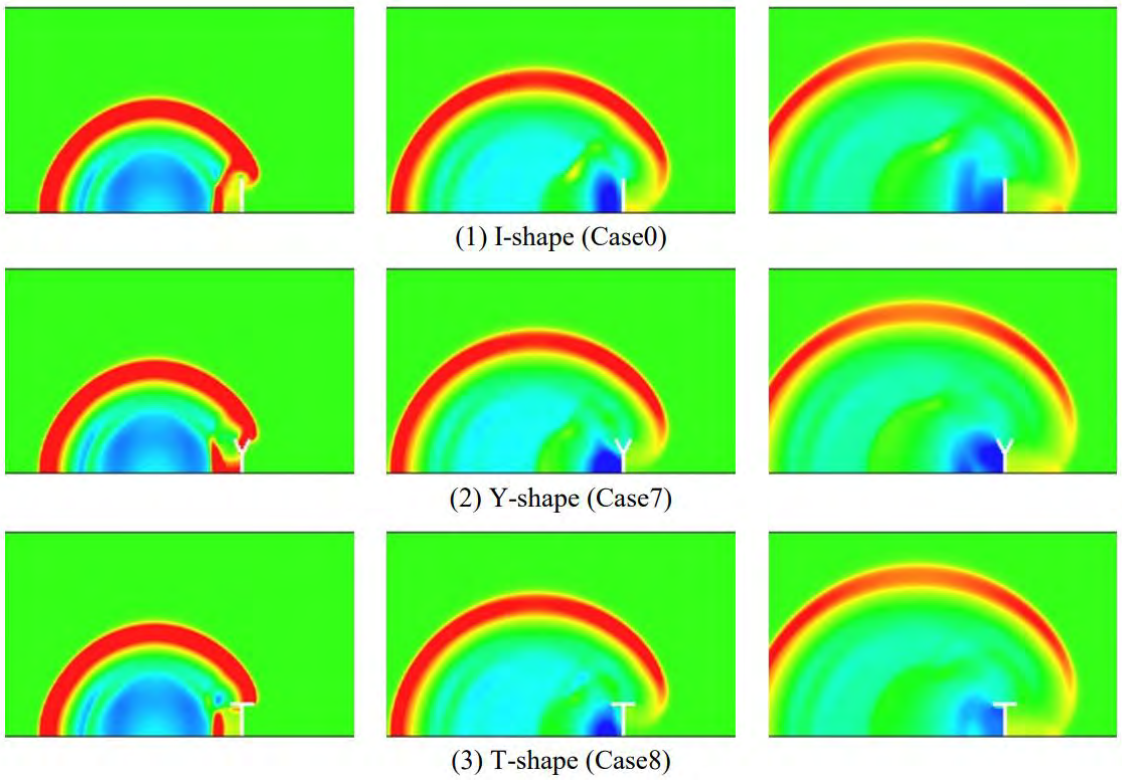

Figure 2-6. Instantaneous Pressure Contours for Walls with I-shape, Y-shape, and T-shape cross-sections [20].

There could be drawbacks to using Y- or T-shaped walls. The tops of both walls provide more surfaces on which precipitation like snow or sleet can accumulate, which could compromise the structural integrity of the wall. In addition, if the hydrogen leak is close enough to either wall, the angle between the vertical section and the arms of the alternatively shaped walls could provide a point at which hydrogen could potentially accumulate. Relevant safety standards like NFPA 2 contain guidance regarding allowed numbers of walled surfaces and angles between them, which is an aspect to be considered if implementing a wall geometry other than an I-shape.

Alshammari et. al. studied the impacts of free-standing cylindrical barriers on blast impulse mitigation [24]. It was determined that factors including cylinder position and size as well as the blast wave strength all contributed to the blast mitigation capabilities. Like the conclusions made about the efficacy of solid barriers, the authors found that placing the obstacle closer to the overpressure origin "substantially improve[d] attenuation." They observed that increasing the cylinder diameter led to lower impulse values in a larger area. In addition, the blast energy itself affected the overpressure attenuation qualities of the cylindrical obstacle: more energetic explosions with higher Mach numbers and shock speeds resulted in a larger mitigation area downstream of the obstacle. The authors speculate that this result stemmed from the higher vorticity of fast-moving particles causing reductions in kinetic energy and pressure. Compared to traditional blast barriers with rectangular cross-sections, the area of blast mitigation from a cylindrical obstacle is much smaller and the impulse is not evenly or symmetrically distributed, as shown in Figure 2-7(a). Therefore, while cylindrical obstacles may assist with blast mitigation, a traditional barrier wall would likely provide more protection from explosions. At a hydrogen facility, already-existing cylindrical

obstacles such as bollards may help attenuate overpressure but perhaps not enough for them to be used as the only form of blast mitigation.

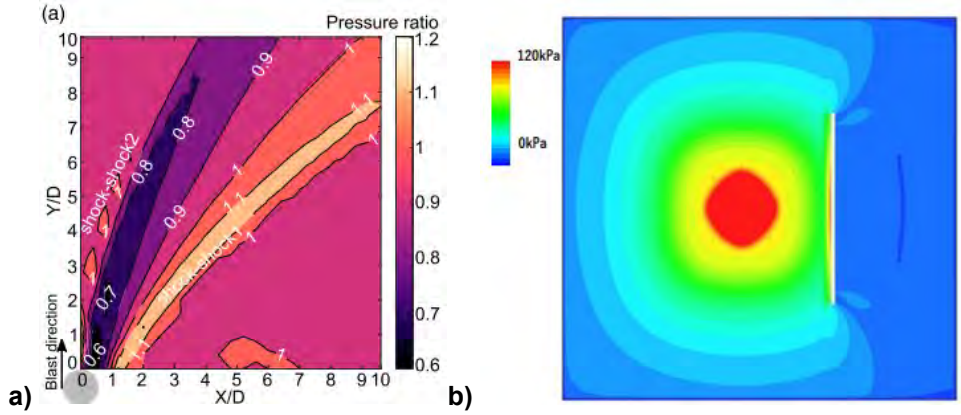

a) b)

Figure 2-7. Birds-eye view of a) peak overpressure downstream of a cylindrical obstacle [24] and b) overpressure contours around a barrier wall [20].

2.3.2.2. Porous Barriers

Several studies have also been published on the use of metal perforated plates for blast mitigation. Much of the available literature investigates the effects of hole geometry and size on downstream overpressure attenuation; examples of tested perforated plates are provided in Figure 2-8.

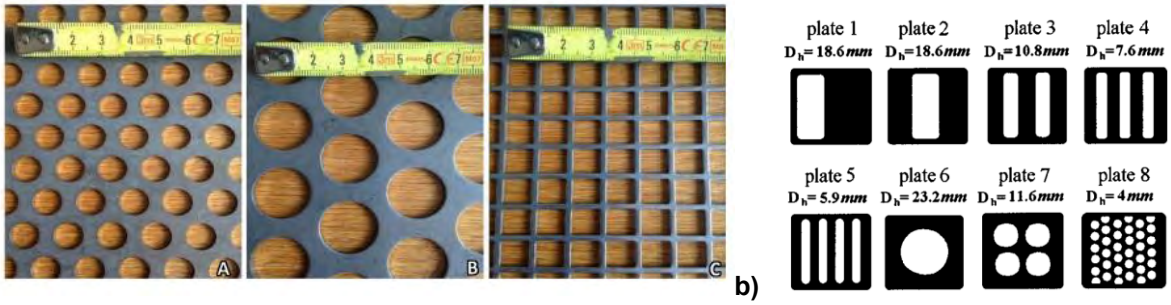

a) b)

Figure 2-8. Example perforated plate hole shapes tested in referenced papers a) [25], b) [26].

Most sources agree that the plate porosity, has a larger impact on the blast mitigation capability of a perforated plate than the hole geometry [25], [27], [28], [29]. Langdon et. al. refers to porosity in terms of blockage ratio, defined as

$$BR = \frac{A_{Perf}}{A_{Exp}}, \qquad \textbf{Equation 2-1}$$

where A_{perf} is the total solid area on the plate face and A_{exp} is the exposed, or open area of the plate face. When the tested blockage ratio was too low – in other words, when the plate porosity was too high – the overpressure and impulse attenuation was not substantial. When perforated plates with higher blockage ratios were used in the study, the target plates downstream of the perforated plates deflected less and experienced tearing at higher impulses, indicating lower degrees of blast damage. Therefore, plates with lower porosity were found to provide better overpressure protection for downstream objects. This conclusion suggests that single perforated plates may not provide an advantage in blast mitigation over traditional solid walls. In addition to the improved blast attenuation of barriers with more overall solid area, materials for solid walls may be more readily available and the solid walls themselves may be easier to install than perforated plates.

Experiments have also been performed on perforated plate arrays or layers, where several perforated plates are placed consecutively in the blast region. Studies by Schunk and Eckenfels and Ram et. al. found that adding layers of plates improves the overpressure attenuation downstream of the plate array [25], [30]. In terms of compatible plate geometries, according to Ram et. al., adding consecutive plates helps most when the plates have lower porosity [30]. In terms of the effects of distance between consecutive plates, Schunk and Eckenfels did not observe a difference in overall blast mitigation when distance between plates was varied. Both papers also discuss the interactions between consecutive plates and whichever part of the wave is reflected rather than being transmitted through the plates. The reflected shock wave can become trapped between consecutive perforated plates, where it attenuates so that even if some of it gets transmitted through the plate array in either direction, it does so with a lower overpressure than the initial blast. This capability of perforated plates in an array potentially offers something different than a solid barrier or single perforated plate because it attenuates overpressure downstream of the barrier without significantly increasing the upstream overpressure and fire temperature effects in the manner of the solid barrier.

Schunk et. al. tested chain mail as a blast mitigation barrier material and also found that it also worked for downstream overpressure reduction, because some of the shock wave is reflected from the material and interaction with the chain mail introduces turbulence into the transmitted part of the shock wave [29]. While Schunk et. al. came to the same conclusion as previously cited literature regarding the larger influence of porosity than geometry on blast mitigation efficacy, they did find that using mesh with beveled holes improved blast mitigation capabilities. Additionally, the paper points out that mesh provides an advantage over using a solid steel plate for blast protection because the rigidity of a solid steel plate could cause it to deform, tear, and potentially damage whatever it is protecting.

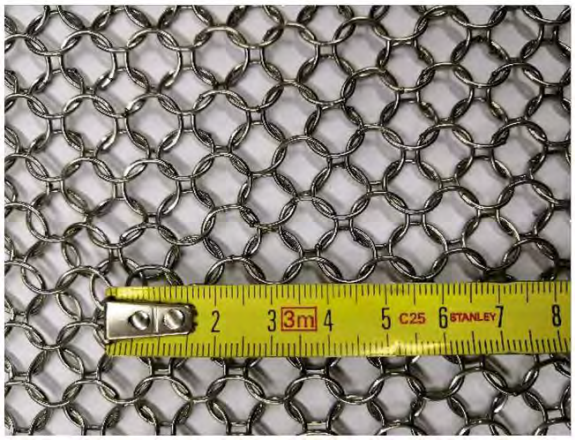

Figure 2-9. Chain mail material used in the experiments conducted by Schunk et. al. [29].

Similarly, Xiao et. al. investigated the efficacy of using woven wire mesh for blast attenuation [31]. They found that the woven mesh did reduce the overpressure at most points downstream except for one location at which the overpressure increased. They also noticed lower maximum impulses downstream of the mesh. The authors acknowledge that the mesh was less effective at mitigating overpressure and impulse than a solid barrier. However, they point out that mesh can be used for some form of blast protection in situations in which it is not possible to install solid walls if they are cost prohibitive or undesired by the public. Mesh and chain mail is light and flexible, which also suggests it may be more portable than other blast mitigation materials like concrete or steel walls, or even steel perforated plates anchored on the ground.

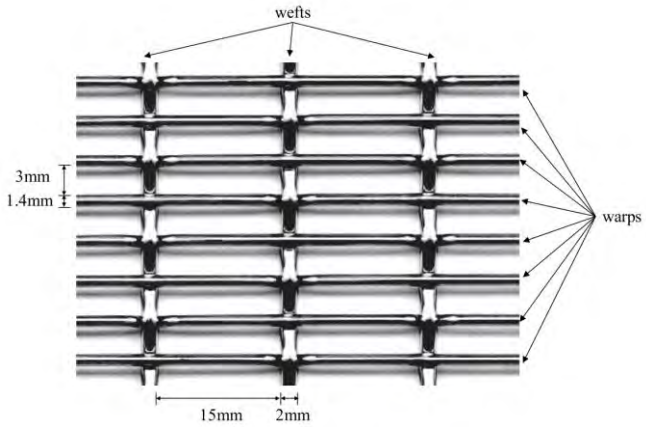

Figure 2-10. Woven wire mesh used in the experiments conducted by Xiao et. al. [31].

2.3.3. Alternative Blast Barrier Materials

2.3.3.1. Water

In the previous section, the studies sought to understand the effects of geometry on the blast mitigation capabilities of a barrier. In this section, material properties are utilized for blast protection.

Water in various wall-like configurations has been proposed as a barrier material. Chen et. al. tested a configuration in which thin plastic bags filled with water were hung inside a steel frame and subjected to an explosion [32]. Like the water deluge method discussed in Section 2.2, the water wall is able to mitigate the explosion through heat effects (i.e., the transfer of blast energy into either internal energy of the water or evaporation of the water) and momentum extraction effects (i.e., the transfer of blast energy into kinetic energy of water droplets). In this setup, there is also a defined water boundary which can also transmit, reflect, and diffract the blast wave, similar to the behavior of a solid barrier. This experiment resulted in an overpressure and impulse reduction downstream of the water wall. The authors found that the water wall became more effective at downstream overpressure mitigation when it was taller and closer to the overpressure origin, which also shows how its properties are similar to that of a solid barrier wall. The water wall would likely be low-cost because it only consists of a steel frame, plastic bags, and water, although the water would of course require replacement after rupturing during an overpressure event. The paper acknowledges the potential downside of acceleration of splashed water by the blast wave; these fast-moving water droplets could cause secondary injury to people even if they are downstream of the water wall.

Figure 2-11. Top-down photo of water wall used in experiments conducted by Chen et. al. [32].

Schunk et. al. also studied a water wall, but one created by a water curtain over the chain mail metal grid shown in Figure 2-9. They found that water flowing over the metal grid created a water wall that reflected the shock wave and attenuated the downstream overpressure and impulse. Unlike the water wall studies done by Chen et. al., the experiment by Schunk et. al. showed that enhancement of the shock wave reflection by the water wall was the most significant behavior; the momentum extraction and heat effects of water forming droplets and evaporating were speculated to be much less instrumental to the blast attenuation.

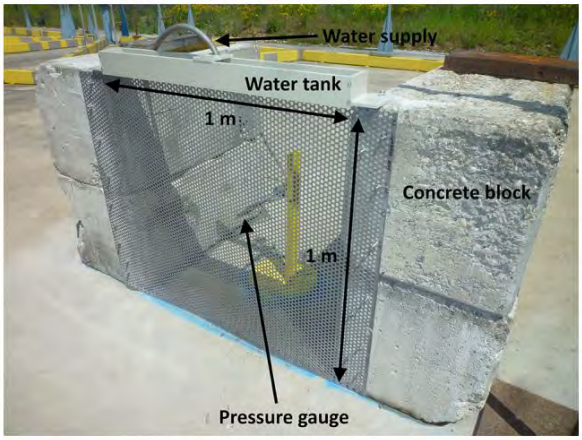

Figure 2-12. a) Chain mail grid and b) water curtain over metal grid setup used in experiments by Schunk et. al. [29].

2.3.3.2. Granular Materials

Filters containing granular materials have been proposed for shock wave attenuation. Granular materials include sand, rock particles, plastic or glass spheres, polystyrene, and nylon [33], [34]. This solution is different from the method discussed in Section 2.2 that also involves granular materials, because this method involves using filters containing granular materials as barriers against a blast wave, instead of using the granular materials to suppress or quench the blast wave. Filters with materials like sand or rock have been used in the past for blast protection [33]. Britan et. al. also characterized the overpressure reduction when using engineered granular materials like plastic and glass spheres of a known uniform size. They conclude that the granular material filters can be made more effective by using particles with smaller diameters and lengthening the filters in the direction of the shock wave.

2.3.3.3. Sacrificial Claddings

Ample literature is available on sacrificial claddings, which "consist of crushable core sandwiched between two thin plates" [35], as shown in Figure 2-13; these are both geometrically and materially different from traditional blast barriers discussed previously. When the sacrificial cladding encounters a blast wave, the front plate accelerates towards the rear plate and the core plastically deforms to absorb some of the kinetic energy and reduce the overpressure felt at the rear plate and beyond. The crushable core is often made of a cellular material such as polyurethane foam, since these materials can undergo large plastic deformations under a low constant stress [35] Ousji et. al. found that some minimum thickness is required for the core to be able to absorb the applied blast load.

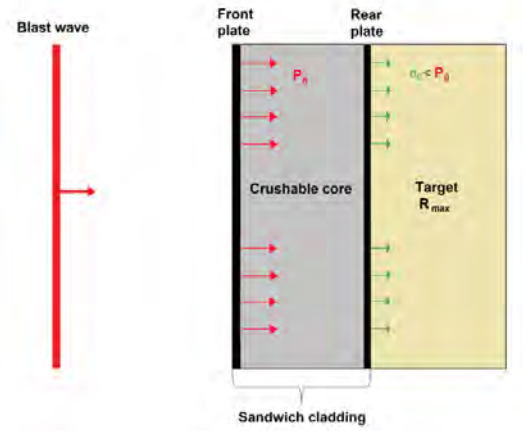

Figure 2-13. Schematic of sacrificial cladding cross-section [36].

The sacrificial cladding can be engineered to enhance its blast attenuation properties. Blanc et. al. published tentative conclusions that galvanizing the polyurethane foam could increase the energy absorption by unit volume [36]. They also found that thicker galvanized coatings increased the density of the foam and potentially allowed for higher energy absorption by unit volume. This finding is novel in that it implies the properties of galvanized polyurethane foam are comparable to those of pure metal foam in a sacrificial cladding, but the galvanized polyurethane is less expensive. Blanc et. al. also observed that galvanizing the foam with a more ductile metal, for example nickel instead of copper, led to a less brittle crushable core and subsequently better energy absorption properties.

Sacrificial claddings have been experimentally proven to reduce overpressures, and they are a viable option for blast mitigation in a hydrogen plant. However, since the core undergoes plastic deformation when encountering an explosion, a sacrificial cladding cannot be used for multiple blasts and would have to be replaced, which could be more expensive than a more permanent option that can withstand multiple blasts. Additionally, a minimum core thickness is required for the sacrificial cladding to be effective, but this thickness depends on the blast loading, which cannot be anticipated since a leak can happen at multiple points at a facility and the explosion size is not always predictable. If the blast loading were to be underestimated, the core would be too thin and might not provide sufficient protection. If the blast loading were to be overestimated, the core would provide ample protection, but more materials, money, and space may be allocated to the sacrificial cladding than necessary.

2.3.4. Retrofitted Buildings

The methods described in the previous sections show ways that free-standing structures can be used to redirect blast energy and protect people and infrastructure present downstream. Several solutions have been proposed – and some have already been commercialized – for incorporating blast protection directly into infrastructure such as buildings at risk of harm from an overpressure event. Badshah et. al. explains that architectural design can help a building withstand a shock wave [37]. For example, buildings that are limited to one story may sustain less damage than multi-story building. Badshah et. al. also mentions that "Arches and dome shapes attenuate the effect of blast pressure when compared with cubicle or rectangular shapes" [37]. They also point out that increasing building wall thickness, incorporating steel reinforcement, and constantly maintaining and replacing weak components in the building also help. However, they acknowledge that these construction and maintenance decisions may not always be feasible from a financial and temporal standpoint.

Fiber-reinforced composite materials such as carbon fiber reinforced plastic (CFRP), glass fiber reinforced plastic (GFRP), aramid fiber reinforced plastic (AFRP), polyurea, polyurethane, aluminum foam, engineered cementitious composites, and ferrocement have been proposed as reinforcing materials for buildings [37]. Badshah et. al. proposes that composites like CFRP can be used to reinforce masonry walls, and polymers like polyurea can be sprayed on walls to improve blast loading performance, improve flexural strength, and localize mortar joint damage. Composites can be attractive materials for these applications because they are ductile, high strength, and energy-absorbing. The paper also mentions that new structures can also be built using these composite materials. Sastry et. al. performed blast loading experiments on different fiber-reinforced composite combinations like E-glass/epoxy and Kevlar/epoxy with different ply stacking sequences to understand their kinetic energy absorption capabilities [38]. They found the Kevlar-epoxy composite to be the most energy-absorbing out of the tested materials. It was also concluded that the ply orientations of layered composites affected the absorbed energy. These experiments show that composite materials can be engineered to fine-tune their blast protective qualities.

Buildings with windows can also be retrofitted to protect people from secondary injury caused by projectile debris. For example, companies like Viracon offer glazed or laminated window glass made of materials like silicone and Saflex HP [39]. When the windows experience an impulse from a blast wave and shatter, the broken glass will remain adhered to the plastic lamination instead of also being accelerated into projectiles.

2.3.5. Personal Protective Equipment

There has also been some research done on personal protective equipment (PPE) designed for overpressure events. PPE like hard hats can be worn to protect a person from secondary injury caused by flying debris, or in the case that they are thrown against an object by the blast wave and experience a head impact. However, the blast wave itself can also cause significant harm to a person; high overpressures may lead to a sudden high volume of blood flowing to vital organs like the heart and the brain, resulting in effects like high intracranial pressure [40]. These events can cause life-threatening and chronic conditions like traumatic brain injury (TBI) and post-traumatic stress disorder (PTSD).

Chen et. al. proposes using body armor in the form of water-filled tubes for protection against blast loading. When the body armor encounters the blast wave, the end caps on the bottoms of the tubes

open to release the water, causing the blast wave energy to be transferred into the hydraulic energy of the water rather than hydraulic movement of blood in the person's body.

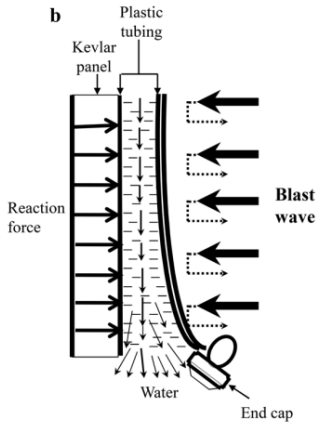

Figure 2-14. Schematic of personal protective armor that redirects blast energy into hydraulic energy during an explosion [40].

Using personal protective equipment (PPE) may be advantageous to use depending on the situation. Since it is portable, it can protect a person from sudden overpressure events if they do not have enough time to move to a less-affected location. However, it can be cumbersome to wear, and can cause fatigue or complacency if operators or workers are expected to wear it all the time even though the probability of an overpressure event at a hydrogen plant is low. Therefore, PPE should only be used if deemed necessary and effective for each individual application. Additionally, the body armor described in this section is just an example and is currently at a low technology readiness level; PPE should only be used in a facility under construction or operation if it has undergone the standard rating and approval processes.

2.4. Discussion of Described Blast Mitigation Techniques

Harm to people and infrastructure from blast loading can be managed in a variety of ways in a hydrogen facility. A hierarchy of controls for hazard and safety management is shown in Figure 2-15.

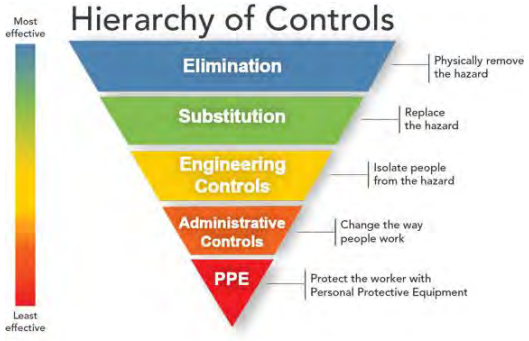

Figure 2-15. Hierarchy of controls [41].

The hierarchy of controls shows that eliminating the hazard is the most effective course of action. For hydrogen facilities, overpressure events can be eliminated by first preventing accidental releases of hydrogen that could mix with air and create a combustible blend. Leak prevention can be

achieved through selection of equipment and materials that can handle and contain hydrogen, and through rigorous leak detection, inspection, maintenance, and repair protocols. Secondly, ignition sources in the area can be eliminated within the facility by using rated electrical equipment and proper grounding and bonding procedures, in addition to signage and training to prevent people from smoking or setting fires in the area. Third, methods such as the blast suppression techniques discussed in Section 2.2 can eliminate the overpressure hazard by quenching the explosion before it propagates towards other parts of the facility.

Even with these elimination methods, there is still some probability of an overpressure event occurring, in which case the hierarchy indicates that engineering controls can be used to isolate people and other equipment or infrastructure from the hazard. The blast isolation and energy redirection methods discussed in this literature survey are both ways of isolating the overpressure hazard and keeping it away from people and other infrastructure.

The hierarchy shows that wearing PPE is the least effective method of hazard management. Although some PPE like the body armor described in the previous section has been proven to work in the event of an explosion, if used, it should not be relied upon as the main source of overpressure protection for people in the facility.

Selecting a blast mitigation method for a hydrogen facility depends on many factors, including the layout and design of the system, whether it is located indoors or outdoors, financial scope, and whether operators will be present or if the system will mostly be self-sufficient. In addition, applicable safety codes and standards can be informative of which blast mitigation technologies are allowed or preferable.

3. CATASTROPHIC TANK FAILURE ANALYSIS

A catastrophic tank failure analysis was performed for a common hydrogen cylinder. Overpressure was estimated using a TNT equivalence model and blast curves. The TNT equivalence model estimates the chemical contribution to overpressure from combustion of the hydrogen in the cylinder. The blast curves estimate the mechanical contribution to overpressure from the expansion of pressurized gas, accounting for the cylinder geometry.

Previous experiments and analysis with these methods demonstrated that the models are conservative on average [42].

3.1. Cylinder Characteristics

The hydrogen cylinder used in the overpressure calculations had the characteristics defined in Table 3-1.

Table 3-1 Defined parameters for the hydrogen cylinder overpressure calculation

Characteristic	Value
Diameter	782 mm
Length	2753 mm
v_1 = Volume	0.994 m^3
p_1 = Vessel Pressure (absolute)	5091.02 psi (35.1 MPa)
p_0 = Ambient Pressure	14.7 psi (0.10 MPa)
H_2 Mass	23.9 kg
Temperature	15 °C

3.2. Mechanical Contribution to Overpressure Calculation

The mechanical contribution to overpressure was estimated using the method in [43]. Overpressure estimates were produced for positions from 1 m to 1000 m from the cylinder in increments of 1 m.

The calculation is defined by the following overall steps:

1. Calculate the energy
2. Scale the input distances based on the energy calculation
3. Use the scaled distance to obtain scaled overpressure predictions for a spherical pressure vessel from existing overpressure curves
4. Apply an adjustment factor to adjust this overpressure for shape effects
5. Un-scale the scaled overpressure estimates

The first step in the mechanical contribution calculation, the calculation of energy, is performed using Brode's formula [44, 45]:

$$E = \frac{2(p_1 - p_0)v_1}{\gamma_1 - 1} \qquad \text{Eq. 3-1}$$

where p_1 (MPa) is the pressure (absolute) in the cylinder, p_0 (MPa) is the ambient pressure, v_1 is the volume of the cylinder (m^3), and γ_1 is the ratio of specific heats of hydrogen gas. Multiplication by 2 accounts for energy reflected off the ground (ground burst). There are alternate methods for calculating the energy, which depend on which thermodynamic assumptions are made. There is significant uncertainty about which set of thermodynamic assumptions best match reality, but Eq. 3-1 is among the more conservative (higher energy estimate) methods [46].

The ratio of specific heats of hydrogen gas is $\gamma_1 = 1.41$. Substituting this value and the other parameter variables from Table 3-1 into Eq. 3-1 gives an internal energy estimate of 169.71 MJ.

The second step in the mechanical contribution calculation scales the distances at which the overpressure is to be estimated ($R \in \{1,2,3, \ldots 1000\}\, m$) based on the internal energy calculation in the previous step. The expression for this scaling is [45]:

$$\bar{R} = R\left[\frac{{p_0}^{1/3}}{E^{1/3}}\right] \qquad \text{Eq. 3-2}$$

The scaled distances from this expression are shown in Figure 3-1.

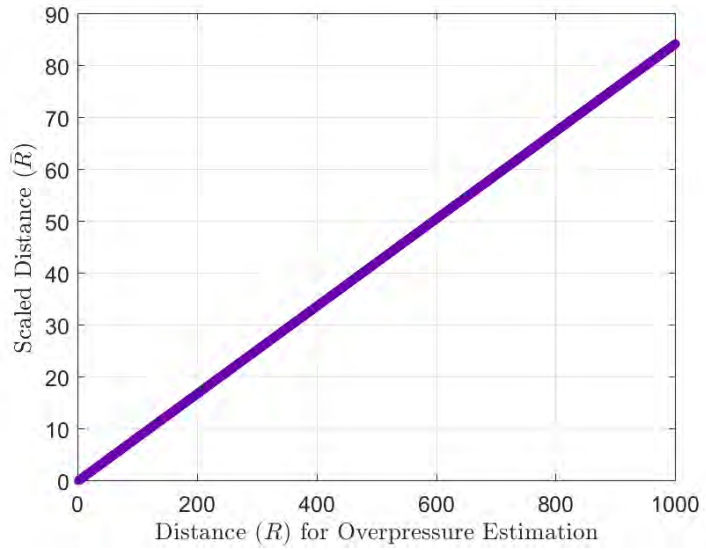

Figure 3-1 Scaled distances for mechanical contribution to overpressure

The third step in the mechanical contribution calculation is to estimate overpressure as a function of the scaled distance from blast curves for spherical pressure vessels. The Baker-Tang blast curves for pressure vessel bursts in [45] were used. Separate curves are provided in [45] for ratios of vessel to

ambient pressure $p_1/p_0 = \{5, 10, 20, 50, 100, 200, 500, 1000\}$. For this analysis, that ratio is $p_1/p_0 = 346.33$. The level of graphical fidelity in the published blast curves makes interpolation between the curves unreliable, so the curve for $p_1/p_0 = 500$ was used. This leads to slightly higher overpressure predictions near the cylinder and slightly lower overpressure predictions farther from the vessel than would be expected at $p_1/p_0 = 346.33$.

Additionally, the blast curve only extends to a scaled distance of 10 and scaled overpressure values were needed up to a scaled distance of $\bar{R} = 84.21$. Extrapolation this far beyond the support of the blast curve may be unreliable so the overpressure value at $\bar{R} = 10$ was used for all $\bar{R} > 10$. Because overpressure decreases monotonically with distance, this is a conservative assumption.

Scaled overpressure values were estimated from this blast curve by first digitizing the plot [47] and then linearly extrapolating [48] at each $\bar{R}$ from Eq. 3-2. The digitized curve and interpolated and extrapolated points are shown in Figure 3-2.

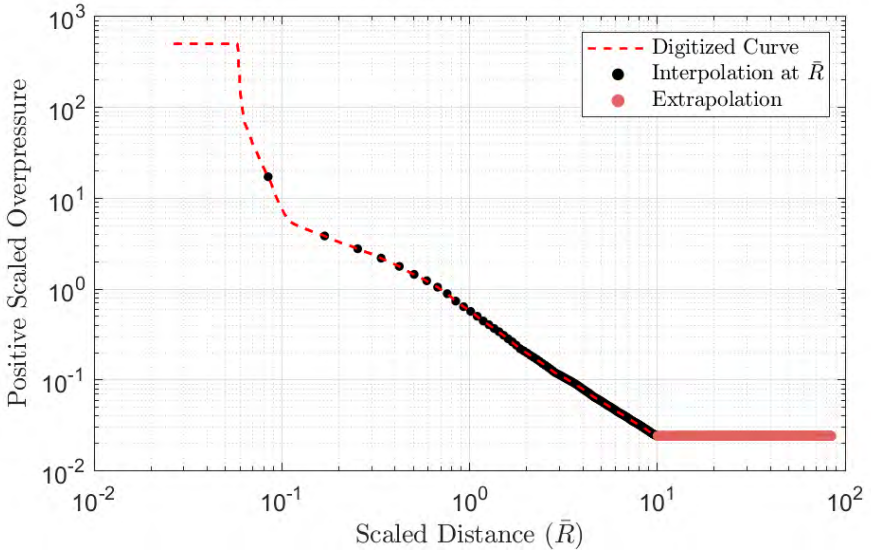

Figure 3-2 Digitized scaled positive overpressure curve with interpolated points

The fourth step in the mechanical contribution calculation is to modify the positive scaled overpressures obtained in the previous step to account for directional effects from the cylindrical shape of the pressure vessel. This adjustment is based on the aspect ratio of the cylinder length to diameter and the orientation of the cylinder. Adjustment factor (overpressure ratio) curves exist [45, 49] for a cylinder in free air and can be applied to cylinders on the ground by modifying the cylinder dimensions. For a cylinder with length L and diameter D, the equivalent dimensions for a cylinder stored vertically on the ground are $2L$ and D. For the same cylinder stored horizontally on the ground, the equivalent dimensions are L and $D\sqrt{2}$. Hence, the actual aspect ratio for the cylinder is $L/D = 2753/782 \approx 3.5$, but the overpressure ratio used for the vertical orientation corresponds to a free air cylinder with aspect ratio $2L/D = 2 * 2753/782 \approx 7$ and the overpressure ratio used for the horizontal orientation corresponds to a free air cylinder with aspect ratio $L/D\sqrt{2} = (2753)/782(\sqrt{2}) \approx 2.5$.

Overpressure ratio curves from Geng et al. [49] are for free air cylinders with aspect ratios $L/D = \{1, 2, 5, 10\}$. These curves present the overpressure ratios as a function of scaled distance ($\bar{R}$) for vessels with different pressures. The curves for $L/D = 5$ were used to obtain the overpressure ratios for the cylinder in a horizontal orientation on the ground. The curves for $L/D = 10$ were used to obtain the overpressure ratios for the cylinder in a vertical orientation on the ground. Using the curve for $L/D = 10$ when $L/D \approx 7$ is the equivalent aspect ratio results in a lower ratio near the cylinder and a larger ratio farther from the cylinder than would be expected at $L/D \approx 7$. Similarly, using the curve for $L/D = 5$ when $L/D = 2.5$ results in a lower aspect ratio near the cylinder and a larger ratio farther from the cylinder.

To obtain the overpressure ratios, the plots for $L/D = 5$ and $L/D = 10$ from [49] were first digitized [47]. Each plot contains an overpressure ratio curve for pressure ratios $p_1/p_0 = \{10, 20, 50, 100\}$ as a function of $\bar{R}$. The pressure ratio for this analysis ($p_1/p_0 = 346.33$) is substantially higher, so using the closest curve $p_1/p_0 = 100$ may not be sufficient. Instead, extrapolation was performed at each $\bar{R}$ value for which overpressure ratios were provided in [49]. This extrapolation is a significant assumption in the analysis. It is possible that extension to cylinders with pressure this high is inaccurate; experimentation is needed to validate the model in this regime.

The digitized overpressure ratios for the cylinder on the ground in a horizontal orientation (free air $L/D = 5$ equivalent) are shown in Figure 3-3. Each arrow illustrates where a monotonic function was fit to extrapolate to the higher-pressure cylinder. Note that by $\bar{R} = 0.8$, the curve for p_1/p_0 is still a decreasing function with respect to p_1/p_0. However, the inflection points for the other pressure ratio curves are at lower $\bar{R}$. Because of this, the point for the p_1/p_0 curve was treated as an outlier at $\bar{R} = 0.8$ and was excluded from the extrapolation. Though this further limits the amount of data used for the extrapolation, the point being excluded is the least applicable point to the high-pressure cylinder we are modeling.

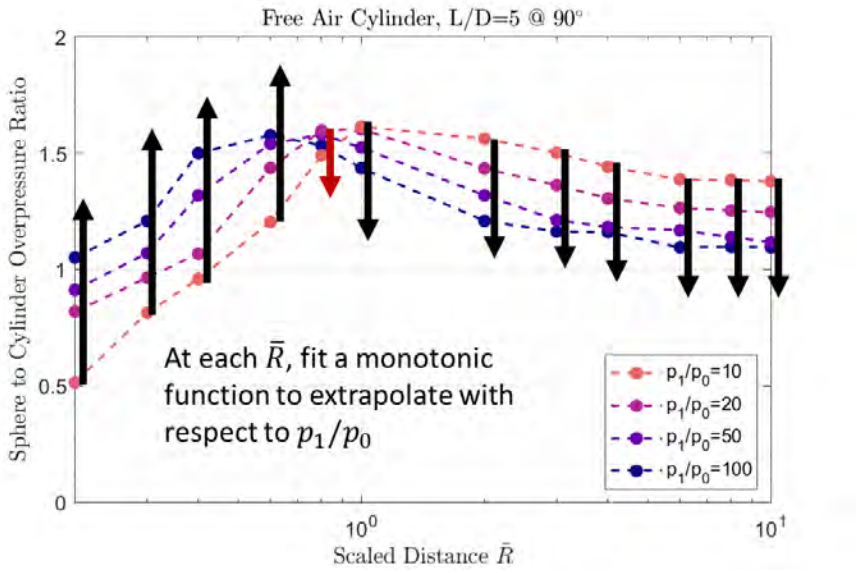

Figure 3-3 Digitized overpressure ratios from [49] for $L/D = 5$ illustrating independent extrapolations with respect to p_1/p_0 for each $\bar{R}$ value; the red arrow indicates where points were excluded from the extrapolation

The corresponding plot for the cylinder on the ground in a vertical orientation (free air $L/D = 10$ equivalent) is shown in Figure 3-4. For this case, two points ($p_1/p_2 = 10$ and $p_1/p_2 = 20$) had to be excluded from the extrapolation at $\bar{R} = 10$ because of the unaligned inflection points in the curves.

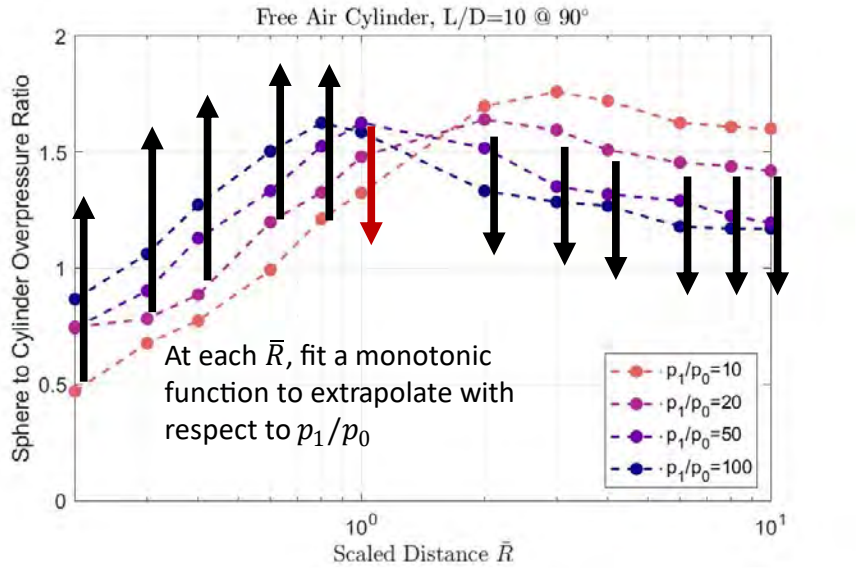

Figure 3-4 Digitized overpressure ratios from [49] for $L/D = 10$ illustrating independent extrapolations with respect to p_1/p_0 for each $\bar{R}$ value; the red arrow indicates where points were excluded from the extrapolation

Figure 3-5 shows each extrapolation model for the horizontal orientation case (Figure 3-3) and Figure 3-6 shows each extrapolation model for the vertical orientation case (Figure 3-4). The fitted models are first order power functions and show good agreement at most points. A power function

was used because of its monotonicity, the log scale of the points, and the reasonableness of the resulting fits given the small sample size. The extrapolated point for $\bar{R} = 0.2$ in Figure 3-6 may be too high because the point at $p_1/p_0 = 10$ is causing the power function to be steeper than may be indicated by the other three points. However, there is limited information to make an informed judgement about excluding the point or choosing a different model, so this value is included in the final extrapolated curve and may be conservative.

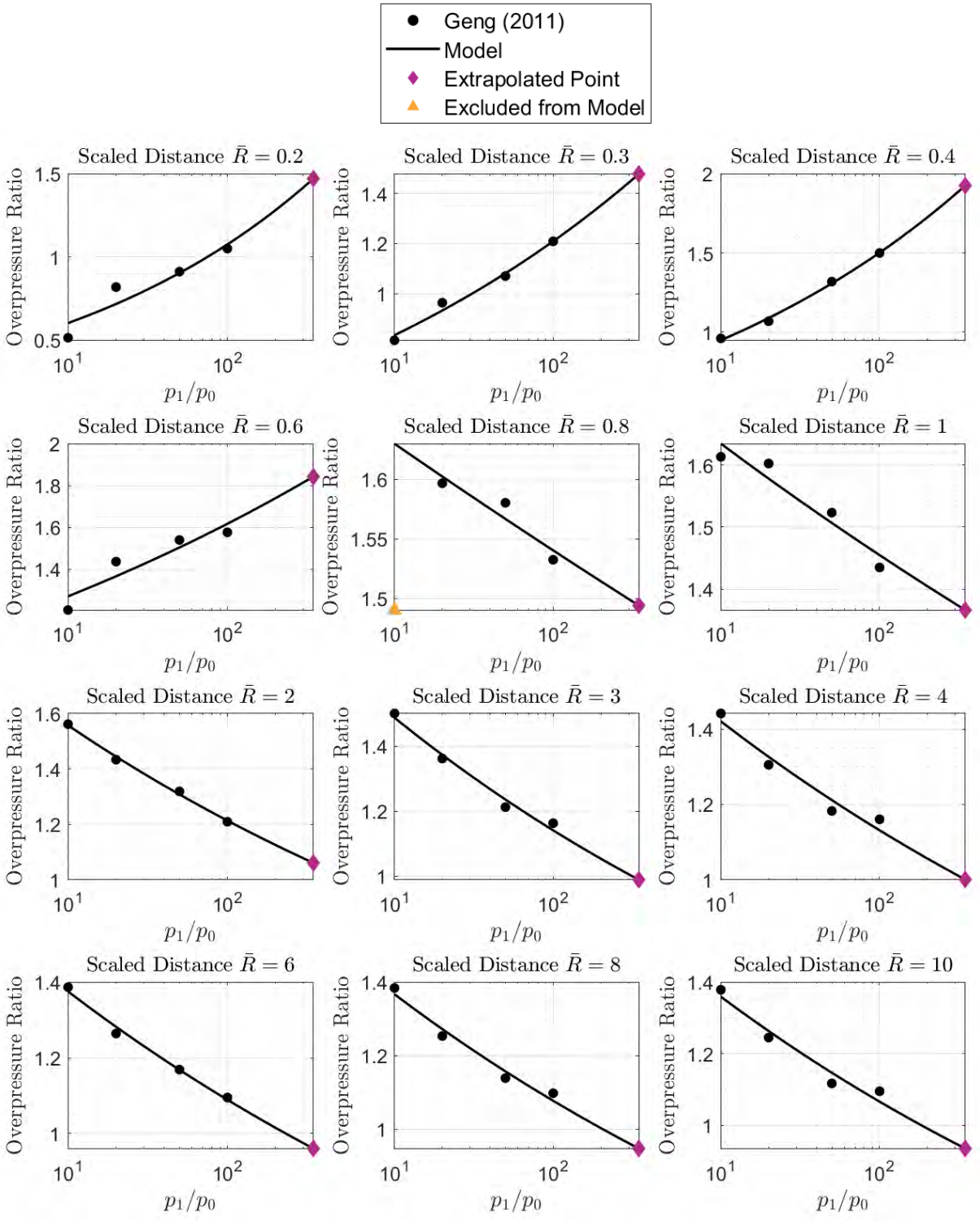

Figure 3-5 Free air cylinder overpressure ratio curves extracted from [49] with fitted power function and extrapolated point at $p_1/p_0 = 346.33$ for cylinder on the ground in a horizontal orientation

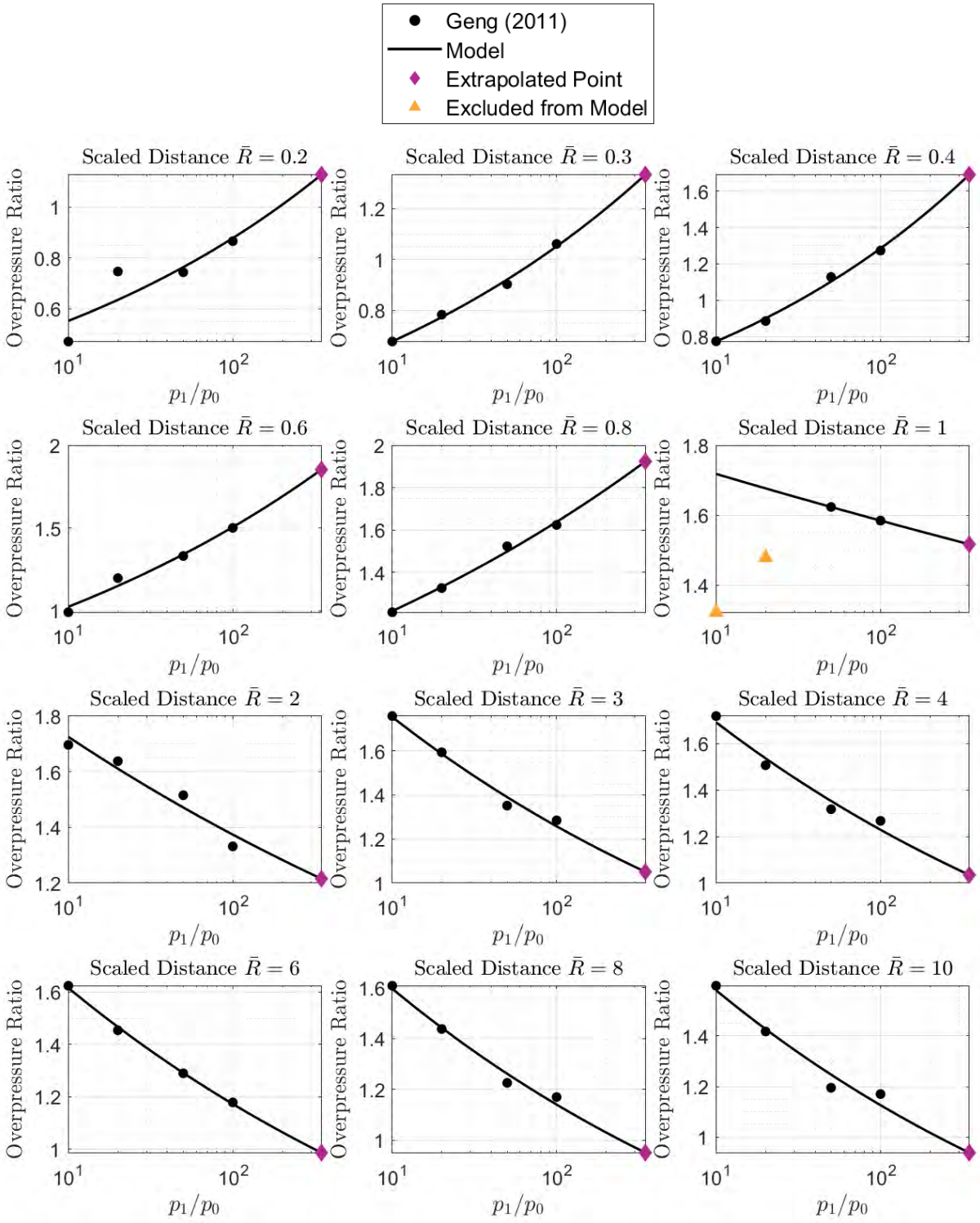

Figure 3-6 Free air cylinder overpressure ratio curves extracted from [49] with fitted power function and extrapolated point at $p_1/p_0 = 346.33$ for cylinder on the ground in a vertical orientation

The full extrapolated overpressure ratio curve for $p_1/p_0 = 346.33$ is shown with the curves from [49] for the horizontal case in Figure 3-7 and for the vertical case in Figure 3-8. The extrapolated curves appear reasonable, especially at scaled distances great than $\bar{R} = 1$, but the appropriateness of the extrapolation cannot be established without further validation in this regime. There is higher uncertainty about the location and magnitude of the inflection point in the extrapolated curve.

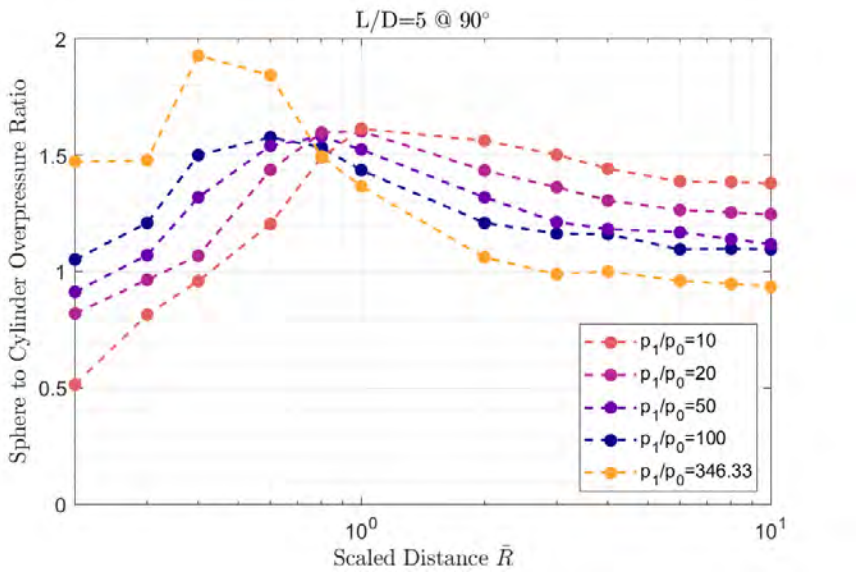

Figure 3-7 Final extrapolated overpressure curve for the horizontal cylinder case ($L/D = 5$ free air equivalent)

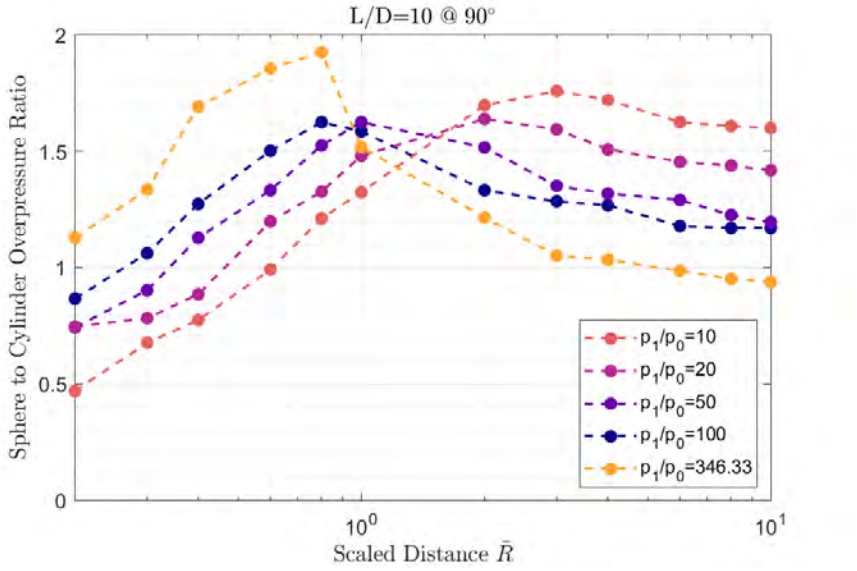

Figure 3-8 Final extrapolated overpressure curve for the vertical cylinder case ($L/D = 10$ free air equivalent)

These overpressure ratios were multiplied by the scaled overpressure estimates in Figure 3-2. The resulted adjusted scaled horizontal cylinder overpressure estimate is plotted against the spherical pressure vessel estimate in Figure 3-9 (left); the plot for the vertical orientation is shown in Figure 3-9 (right). This comparison shows the effect of the vessel shape on the mechanical contribution to

overpressure. Near the cylinder, the overpressure perpendicular to the length of the cylinder is slightly lower than would be expected from a spherical vessel, but higher overpressures are seen farther from the cylinder than would be expected from a spherical vessel. The results are similar between the two orientations.

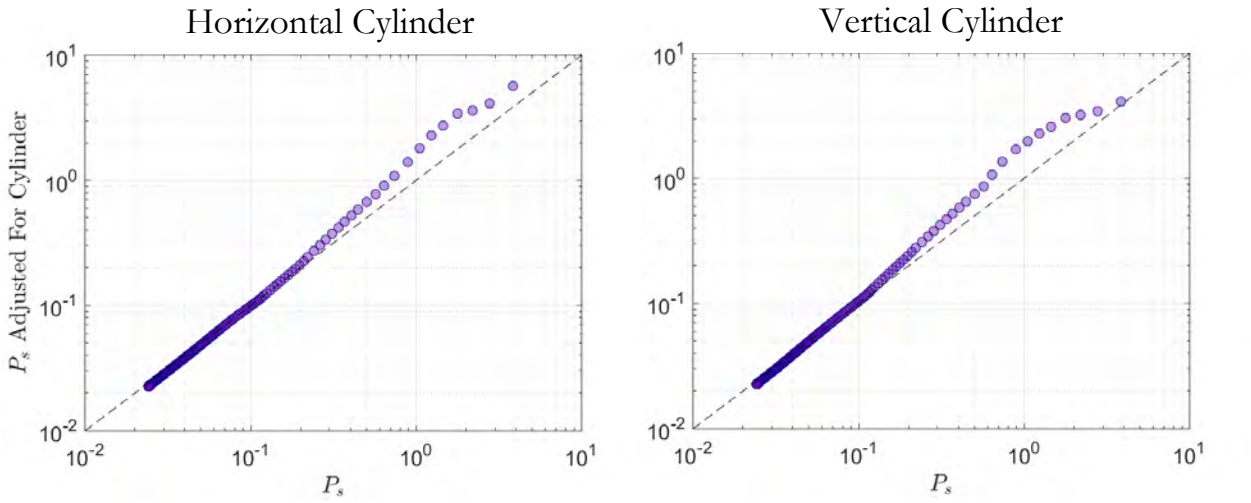

Figure 3-9 Scaled positive overpressure estimates for the cylinder versus spherical vessel estimates

The final step in the mechanical overpressure calculation is to un-scale the adjusted overpressure estimates. The scaling was only performed to standardize the problem for generic blast curves, the resulting overpressure estimates need to be unscaled to return to the original problem space. This is done by multiplying the scaled overpressure by the ambient pressure [45].

The final mechanical contributions to overpressure are shown in Figure 3-10.

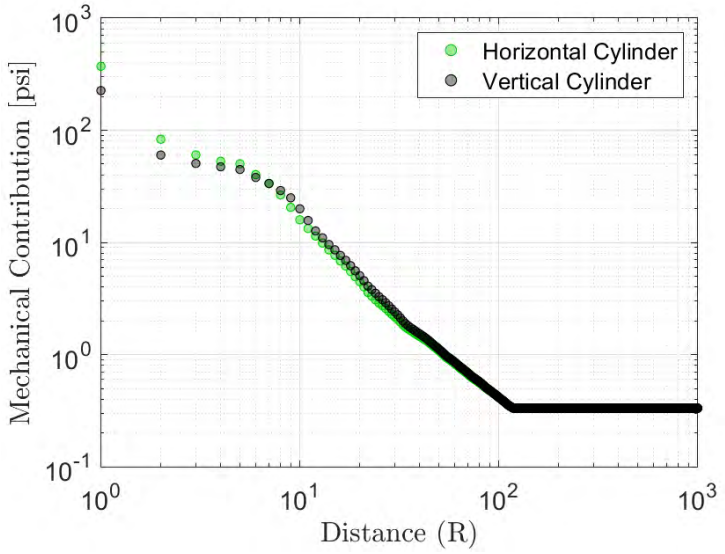

Figure 3-10 Estimates for the mechanical contribution to overpressure for cylinders on the ground in horizonal and vertical orientations

3.3. Chemical Contribution to Overpressure Calculation

The chemical contribution to overpressure was estimated using the TNT equivalency method [43] in the following steps:

1. Calculate the TNT equivalence factor
2. Use the TNT equivalence factor to calculate scaled distance
3. Read the chemical contribution to overpressure from blast curves as a function of scaled distance
4. Un-scale the scaled overpressure estimates

The TNT equivalence factor was calculated as [43]:

$$W_{TNT} = \alpha_e \frac{W_f H_f}{H_{TNT}} \qquad \text{Eq. 3-3}$$

where W_{TNT} denotes the equivalence mass, α_e is the TNT equivalence factor based on energy, W_f is the mass of hydrogen in the cylinder, H_f is the heat of combustion of hydrogen, and H_{TNT} is the TNT heat of detonation. The values for all parameters are listed in Table 3-2. The values used for α_e, H_f, and H_{TNT} are the values in the HyRAM+ (Hydrogen Plus Other Alternative Fuels Risk Assessment Models) software.

Table 3-2 Parameters for the TNT equivalence factor calculation

Parameter	Value	Unit
α_e	0.03	-
W_f	23.9	kg
H_f	120	MJ/kg
H_{TNT}	4.68	MJ/kg

This calculation yields a TNT equivalence mass of 18.38 kg. This value is conservative since it assumes the involvement of all the hydrogen in the cylinder in the reaction.

The second step in the chemical calculation is to scale the distances, $R = \{1,2,3, \ldots 1000\}\, m$, based on the TNT equivalence factor. The expression for scaling from [43] is:

$$\bar{R} = \frac{R}{W_{TNT}^{1/3}}$$

The scaled distances are shown versus R in Figure 3-11.

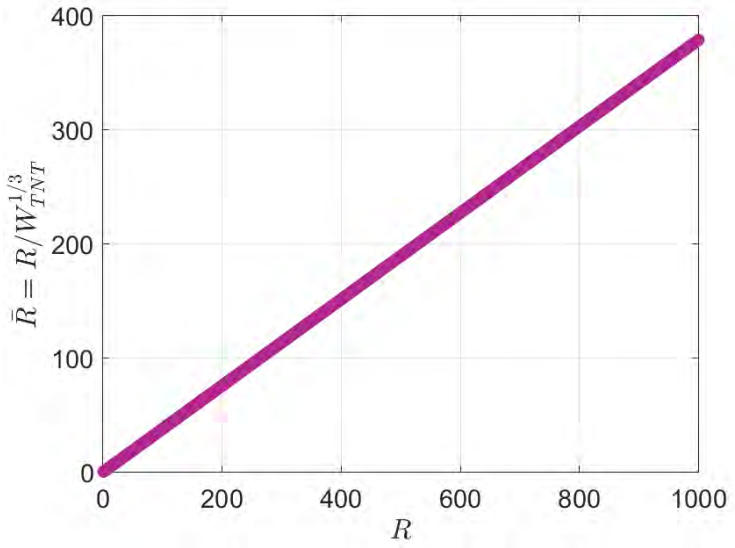

Figure 3-11 Scaled distances plotted versus R for the chemical contribution to overpressure calculation

To obtain the chemical contribution to overpressure, the blast curves from [43] were evaluated at $\bar{R}$. Because these curves have been implemented in HyRAM+, digitization was not required. HyRAM+ was used to interrogate the blast curves for the chemical contribution to overpressure. As with the mechanical contribution calculation, the blast curves are in a scaled (standardized) space. The scaled overpressure estimates were similarly unscaled to obtain the final estimates for chemical contribution to overpressure. The final estimate of the chemical contribution to overpressure is shown in Figure 3-12.

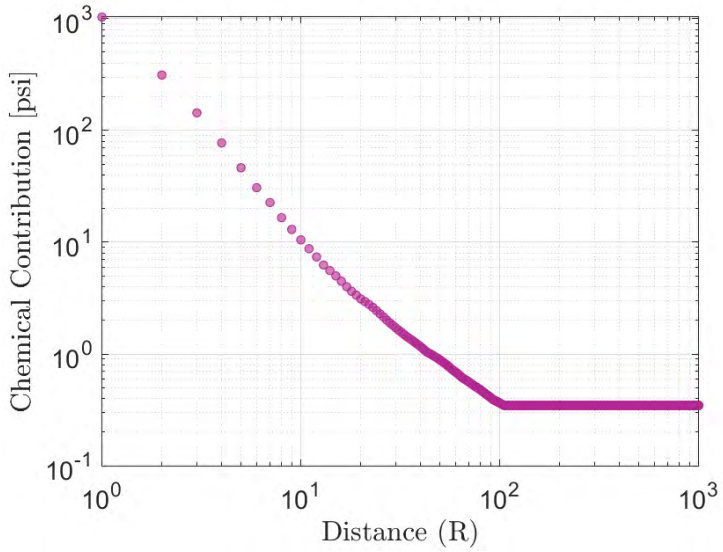

Figure 3-12 Estimated chemical contribution to overpressure from the hydrogen

3.4. Overpressure Results

The final overpressure results are the sum of the mechanical and chemical contributions to overpressure. These are plotted for a cylinder on the ground in both orientations in Figure 3-13. Figure 3-14 (horizontal orientation) and Figure 3-15 (vertical orientation) show the mechanical and chemical contributions separately for each result. These figures illustrate one of the reasons why the results in Figure 3-13 are so similar between the horizontal and vertical cylinders; the chemical contribution to overpressure is significant and there are no orientation effects from this component of overpressure. Additionally, as seen in Figure 3-10, the effect of the cylinder orientation on the mechanical contribution is noticeable but not extreme.

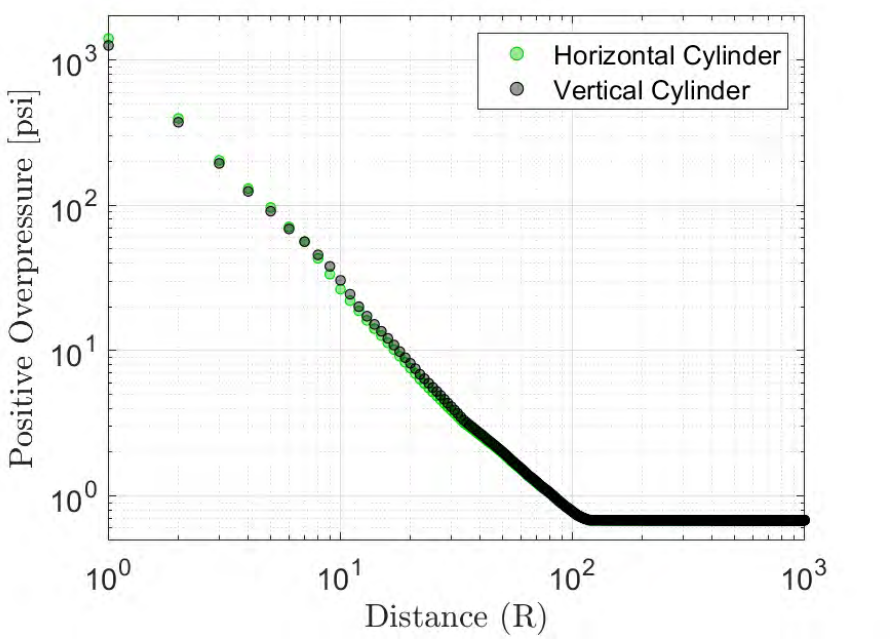

Figure 3-13 Positive overpressure estimates for the cylinder on the ground in a horizontal and vertical orientation

The overpressure estimates include assumptions, such as extrapolating the overpressure ratio curves in the mechanical calculation and including the full inventory of hydrogen in the chemical calculation, that make the accuracy of these estimates uncertain.

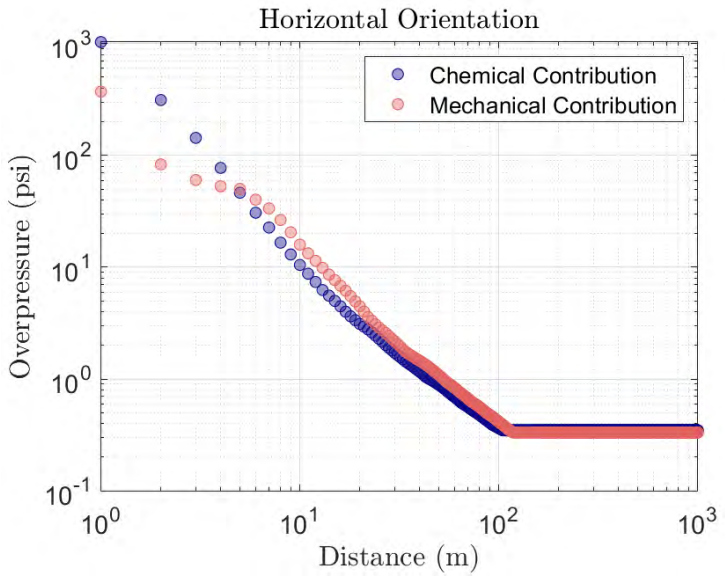

Figure 3-14 Mechanical and chemical contributions to overpressure for the cylinder in a horizontal orientation on the ground

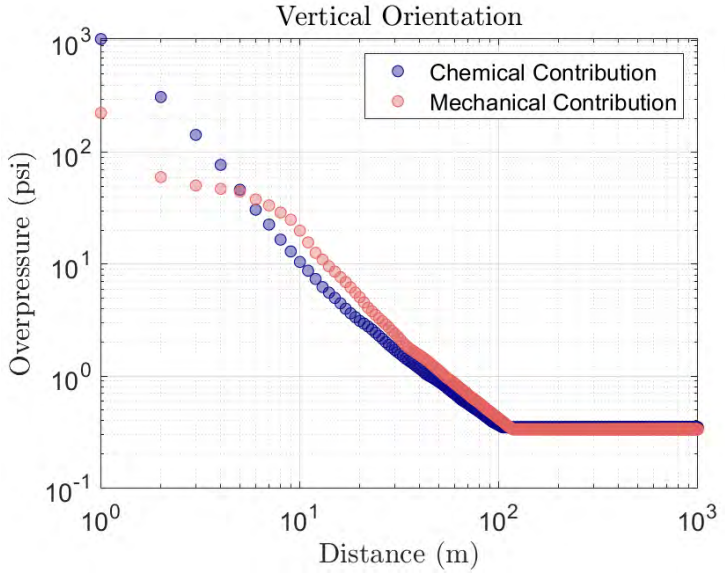

Figure 3-15 Mechanical and chemical contributions to overpressure for the cylinder in a vertical orientation on the ground

4. HYRAM+ AND R.G. 1.91 METHODOLOGY COMPARISON

The HyRAM+ software toolkit [50] was developed by Sandia and integrates data and methods relevant to assessing the safety of the delivery, storage, and use of hydrogen and other alternative fuels. It incorporates experimentally validated models of various aspects of release and flame behavior. HyRAM+ has three different methods for calculating unconfined overpressure: the Baket-Strehlow-Tang (BST) model, the TNT equivalence method, and the Bauwens method. R.G. 1.91 [51] describes the TNT equivalence method as an acceptable method for establishing the distances beyond which no adverse effects would occur based on peak incident overpressure. This section documents a comparison between the methodology prescribed in R.G. 1.91 and HyRAM+ when utilizing the TNT equivalence methodology.

In HyRAM+, there are generally three steps used to calculate the overpressure associated with a vapor cloud explosion scenario. First, the quantity of hydrogen is converted to an equivalent mass of TNT through the following equation:

$$W_{TNT} = \alpha_e \frac{W_f H_f}{H_{TNT}}$$

Where:

α_e is the yield fraction

W_f is the mass of hydrogen

H_f is the theoretical net heat of combustion of hydrogen

H_{TNT} is the heat of combustion of TNT

This is the same for both the methodology prescribed in R.G. 1.91 as well as what is programed into HyRAM+. There is a slight difference in the value of the heat of combustion of TNT: HyRAM+ uses a value of 4.68 MJ/kg while R.G. 1.91 prescribes a value of 4.5 MJ/kg. Also, the heat of combusion for hydrogen is 120 MJ/kg in HyRAM+ while R.G. 1.91 prescribes a value of 130.8 MJ/kg. The yield fraction can be set manually in the GUI in HyRAM+ to any value and R.G. 1.91 prescribes a value of 5%. Additionally, there is additional functionality in HyRAM+ which calculates the quantity of hydrogen for a given leak scenario. R.G. 1.91 allows for the direct input of a known quantity of hydrogen into the TNT equivalence calculations. This is available in HyRAM+ as well. Also, HyRAM+ allows for the calculation of the quantity of hydrogen utilizing its unconfined and unignited jet/plume physics models. This is done by volumetrically integrating the product of the mass fraction and density of the jet/plume that is within the flammability limits. Figure 4-1 shows the jet plume calculated for a hydrogen release in HyRAM+. Note, when utilizing the GUI, HyRAM+ will calculate the quantity of hydrogen from the plume dispersion analysis. A direct input of hydrogen quantity can be accompolished by utilizing the publically available HyRAM+ source code.

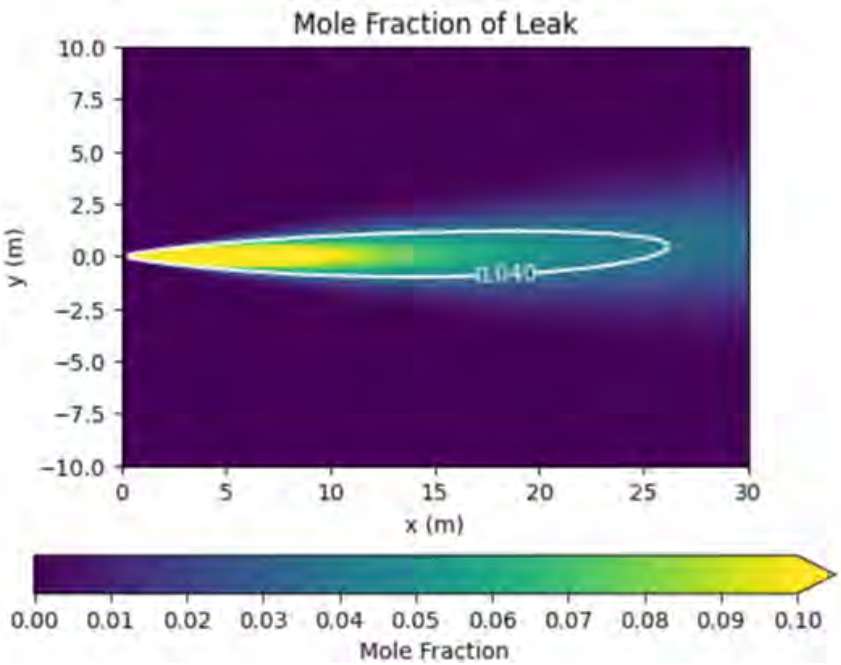

Figure 4-1: Example hydrogen plume calculated in HyRAM+

After the equivalent TNT mass is calculated, the scaled distance is calculated in HyRAM+ utilizing the following equation:

$$R^*_{TNT} = \frac{R}{m_{TNT}^{\frac{1}{3}}}$$

Where:

R^*_{TNT} is the scaled distance
R is the distance from the explosion
m_{TNT} is the mass of TNT

Next, the peak overpressure is determined from a plot. Figure 4-2 shows the scaled peak overpressure vs. scaled distance plot for the TNT equivalence methodology that is utilized within HyRAM+.

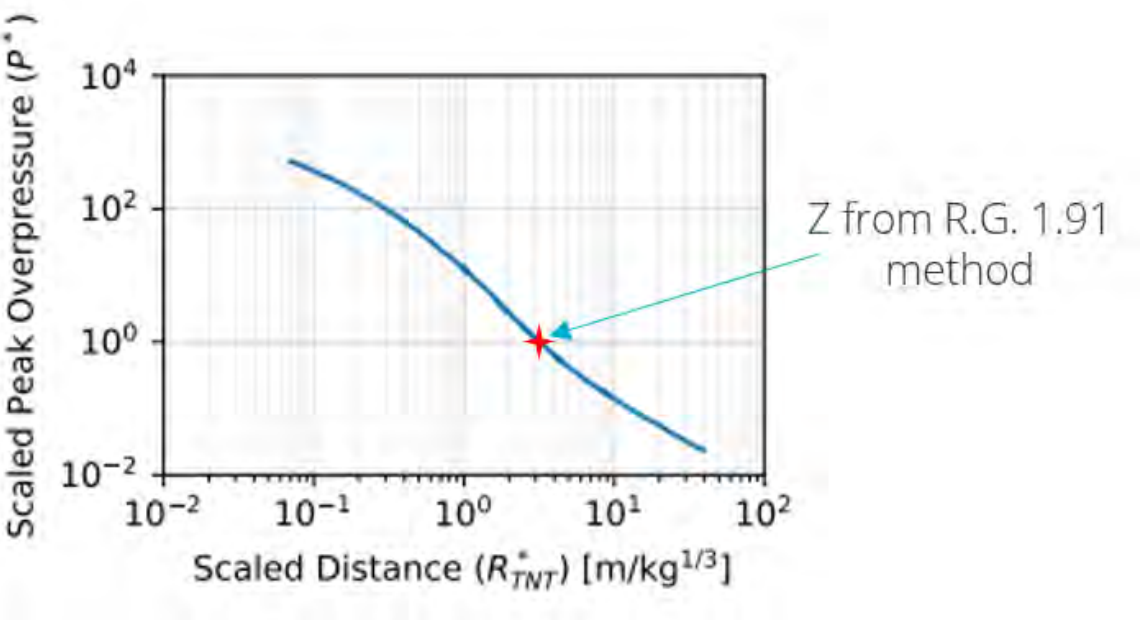

Figure 4-2: TNT Equivalency Blast Curve

Utilization of the blast curve allows HyRAM+ to calculate an Overpressure vs. Distance curve for each given leak scenario. The model prescribed in R.G. 1.91 is essentially identical to the HyRAM+ methodology. However, the equation in R.G. 1.91 only calculates the distance at which the overpressure will equal 1.0 psi. The equations and methodology for executing the TNT equivalency method in R.G. 1.91 is essentially the same as what is programmed in HyRAM+. There are slight differences in some of the input values used in the equations and additional functionality that is available in HyRAM+.

5. SYNGAS PRODUCTION FACILITY CONSEQUENCE ASSESSMENT

As part of the flexible plant operations and generation program at an NPP, synthetic gas (syngas) production is an alternative option to a co-located hydrogen production facility. Syngas is an intermediate product of a synthetic fuel facility, which can be used to produce synthetic liquid fuels. In order for a syngas facility to be co-located with an NPP, the facility would also need to comply with regulatory requirements in terms of consequence safety. In this paper, an overpressure event is evaluated utilizing the TNT equivalence methodology. As with previous studies of overpressure events from a co-located hydrogen generation facility, the fragility of critical components at the NPP is taken to be 1 psi. Therefore, the distance at which the overpressure reaches 1 psi from the detonation location is documented as the result of this calculation.

A preliminary risk analysis of co-located hydrogen and syngas production facilities was performed by Christian, et al [52]. In this report, the properties of syngas during different phases of the production cycle (Process Flow 7 and Process Flow 10) were calculated using Aspen software and the Le Chatelier equation. Additionally, the maximum credible accident (MCA) for syngas was determined to be a pipe rupture during the Process Flow 7 and Process Flow 10. Note, that a comparison of the respective pressure and temperature of the flows to their critical points indicate that Process Flow 7 is categorized as a gas while Process Flow 10 is a categorized as a supercritical fluid. It is assumed that the TNT equivalence methodology is appropriate for both phases of the syngas. The metrics of interest from this analysis are listed below [52]:

- Process Flow 7 for gaseous syngas mixtures
    - Heat of Combustion (kJ/kg) = 7,970
    - MCA total released quantity (kg) = 485.5
- Process Flow 10 for supercritical syngas mixture
    - Heat of Combustion (kJ/kg) = $1.044 * 10^5$
    - MCA total released quantity (kg) = 172.3

These inputs are used in the TNT equivalency methodology outlined in Section 4. Note, for consistency with previous evaluations done for co-located hydrogen generation facilities, the following generic inputs were used in the TNT equivalency calculations. Note, that the equivalence factor used in these calculations is 1. This is the most conservative option, as it assumes that all of the chemical energy from the released syngas contributes to the overpressure event. This is different than what was done previously for hydrogen, as a lower equivalence factor was justified for hydrogen (see Section 4).

- TNT Specific Energy (kJ/kg) = 4,680
- Ambient Pressure (psi) = 14.7
- Equivalence Factor = 1

Figure 5-1 and Figure 5-2 show the overpressure vs distance results for Process Flow 7 and Process Flow 10, respectively. As shown, the overpressure drops below 1 psi at 160 m for Process Flow 7 and at 267 m for Process Flow 10. Process Flow 10 results in a larger overpressure footprint because the Heat of Combustion is so much larger than that of Process Flow 7. Also, as mentioned previously, the equivalence factor of 1 was conservatively chosen for these calculations.

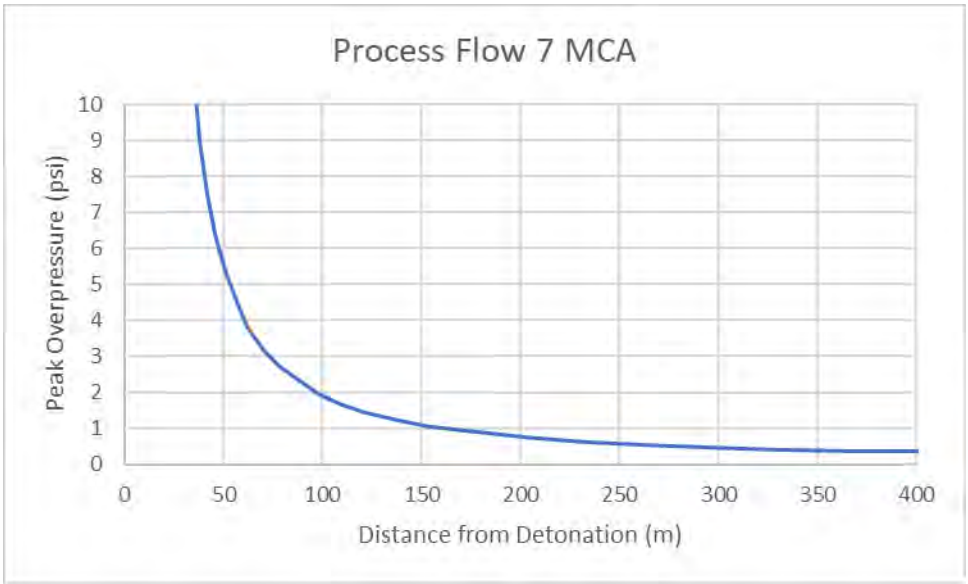

Figure 5-1: Overpressure vs. Distance for Process Flow 7 MCA (Syngas)

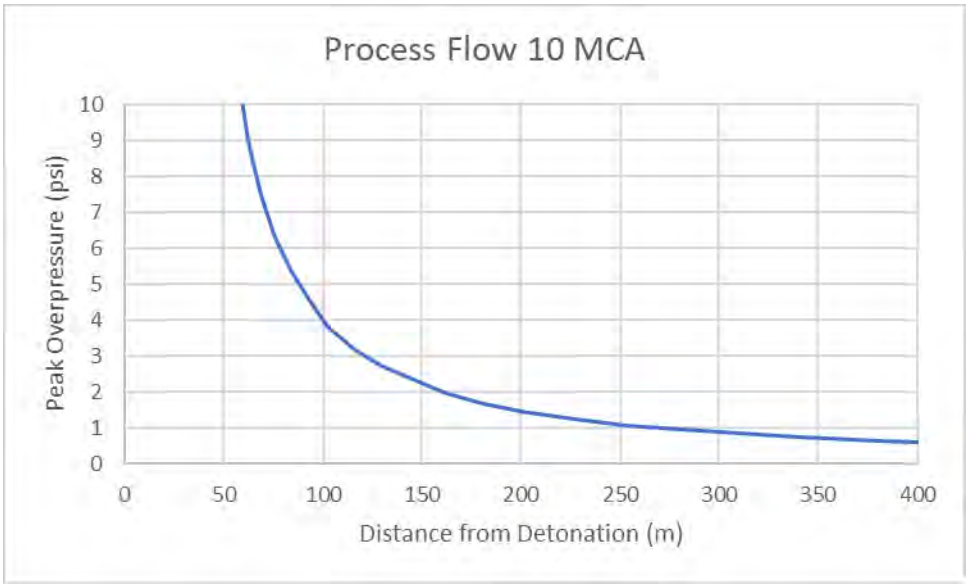

Figure 5-2: Overpressure vs. Distance for Process Flow 10 MCA (Syngas)

6. CONCLUSION

The three overarching categories of blast mitigation methods discussed in this report are methods for blast isolation for the event that a blast has occurred, blast suppression in the event that a blast is imminent, and energy redirection in the event that a blast has occurred.

The blast isolation techniques include passive and active mechanical valves as well as chemical suppression to prevent propagation of the flame to other parts of the system. The commercialized technology for blast isolation tends to be used within vessels and piping. Although any explosions that occur in a hydrogen plant would likely occur in the open air rather than within the system itself, this method can still be considered as an extra protection measure for the internal part of the system.

The blast suppression techniques use materials like water, dry aqueous foams, and dry powders to smother and quench the flame to prevent propagation. In some cases, it can also be used to inert a flammable mixture of fuel and air that has not yet ignited, by increasing the flammability limit. Water mist or spray is a particularly attractive option because it can potentially be incorporated into existing sprinkler system infrastructure, and it is readily available, inexpensive, and nontoxic to people or the environment.

The energy redirection methods are used to reflect, absorb, and diffract energy away from people and infrastructure at risk of harm. The discussed methods are mainly variations on traditional concrete or steel blast barriers. Research has been conducted on different wall shapes, including Y-, T-, and trapezoidal cross-sectional shapes. Some of these geometries show enhanced downstream overpressure attenuation but may take up more space than a traditional I-shaped wall. Literature was also found on different materials for blast energy redirection; water walls, filters filled with granular materials, and sacrificial claddings with foam cores have all been proposed as methods for downstream blast mitigation. Material availability, space constraints, and cost are all factors to consider when determining an appropriate blast energy redirection technology to implement in a particular facility. Besides constructing free-standing barrier-like structures to reduce overpressures, facility designers or owner-operators can also utilize certain materials like composites and laminated windows to strengthen existing or planned buildings. In addition, some PPE has been proven to reduce downstream overpressures and can potentially be used to protect people from biological overpressure harm. While PPE may serve as an extra layer of safety, it is helpful to use it in conjunction with the other blast mitigation techniques.

Informed design of the hydrogen system can help reduce the probability leaking and ignition hazards before they occur, which is a form of blast mitigation. However, the probability of an overpressure event cannot be completely eliminated. Therefore, the overpressure and impulse reduction techniques described in this report can minimize harm to people and infrastructure in case an explosion does happen.

Additionally, a catastrophic hydrogen storage tank failure event was analyzed to determine the resulting overpressure consequence. This event is unique because both the mechanical pressure in the tank as well as the chemical energy contribute to the resulting overpressure. Sensitivity cases were evaluated based on the orientation of the tank to the ground. For both cases, the overpressure drops below 1 psi within 100 meters of the tank location.

The methodology utilized in HyRAM+ was compared to that prescribed in R.G. 1.91. The TNT equivalence methodology to calculate overpressure is used by HyRAM+ and R.G. 1.91. Both methodologies prescribe essentially the same equations. There are some differences in the methodologies, including the values utilized for the inputs into the equations and the method of calculating the hydrogen quantity used in the TNT equivalence methodology.

An overpressure event was also evaluated for a syngas facility. Two scenarios were evaluated, a pipe rupture in different streams of the production process. The maximum credible accident in Stream 10, which contained syngas as a supercritical fluid, was limiting and resulted in a distance of 267 m for the overpressure to drop below 1 psi. Stream 7 contained syngas as a gas and the maximum credible accident resulted in a distance of 160 m for the overpressure to drop below 1 psi.

REFERENCES

[1] IEP Technologies, "Explosion Protection Systems," [Online]. Available: https://www.ieptechnologies.com/whats-the-solution/explosion-protection. [Accessed 12 April 2024].

[2] D. Guaricci, J. Oukhchi and S. Light, "Explosion Isolation Valves," ATEX Explosion Protection, L.P., [Online]. Available: https://atexus.com/ATEXPassive.pdf. [Accessed 12 April 2024].

[3] Boss Products LLC, "Explosion Isolation & Diversion," [Online]. Available: https://bossproductsamerica.com/solutions/fire-explosion-mitigation/explosion-isolation-diversion/. [Accessed 12 April 2024].

[4] M. Gruijicic, B. Pandurangan, C. L. Zhao and B. Cheeseman, "A Computational Investigation of Various Water-Induced Explosion Mitigation Mechanisms," *Multidiscipline Modeling in Materials and Structures,* vol. 3, pp. 185-212, May 2006.

[5] K. van Wingerden, "Mitigation of Gas Explosions Using Water Deluge," *Process Safety Progress,* Vols. 19, no. 3, pp. 173-178, April 2004.

[6] D. Schwer and K. Kailasanath, "Blast Mitigation by Water Mist (3) Mitigation of Confined and Unconfined Blasts," Naval Research Laboratory, Washington D.C., July 2006.

[7] T. Schunk, M. Bastide, D. Eckenfels and J. Legendre, "Blast Mitigation by Water Mist: The Effect of the Detonation Configuration," September 2020.

[8] S. Jones, A. Averill, J. Ingram, P. Holborn, P. Battersby, P. Nolan, I. Kempsell and M. Wakem, "Mitigation of Hydrogen-Air Explosions Using Fine Water Mist Sprays," 2006.

[9] B. Ehrhart, E. Hecht and B. Schroeder, "Hydrogen Plus Other Alternative Fuels Risk Assessment Models (HyRAM+) Version 5.1 Technical Reference Manual," Sandia National Laboratories, SAND2023-14224, December 2023.

[10] S. Dorofeev, "Criteria for FA and DDT Limits".

[11] E. Del Prete, A. Chinnayya, A. Hadjadj and J. Haas, "Blast Wave Mitigation by Dry Aqueous Foams," *Shock Waves,* vol. 23, pp. 39-53, August 2012.

[12] ATEX Explosion Protection, "Dry Chemical System," [Online]. Available: https://atexus.com/corp2/index.php/solutions/85-active-protection-isolation/121-dry-chemical-system.

[13] "Active. Chemical. Suppression," [Online]. Available: https://cvtechnology.com/explosion/chemical-suppression/.

[14] Q. Pontalier, J. Loiseau, S. Goroshin and D. Frost, "Experimental Investigation of Blast Mitigation and Particle-blast Interaction during the Explosive Dispersal of Particles and Liquids".

[15] BDI, "Blast Walls," [Online]. Available: https://www.blastdeflectors.com/blast-walls/.

[16] NFPA, "Hydrogen Technologies Code," 2023.

[17] J. LaChance, A. Tchouvelev and A. Engebo, "Development of Uniform Harm Criteria for Use in Quantitative Risk Analysis of the Hydrogen Infrastructure," *International Journal of Hydrogen Energy,* Vols. 36, no.3, pp. 2381-2388, February 2011.

[18] Block Moulds: benefits of modular construction, "Blast walls," [Online]. Available: https://www.blockmoulds.com/applications/blast-walls/.

[19] C. Gibbons, "What is the Purpose of a Blast Wall?," Blast Resistant Buildings, 18 January 2022. [Online]. Available: https://blog.redguard.com/what-is-the-purpose-of-a-blast-wall.

[20] T. Nozu, R. Tanaka, T. Ogawa, K. Hibi and Y. Sakai, "Numerical Simulation of Hydrogen Explosion Tests with a Barrier Wall for Blast Mitigation," in *International Conference on Hydrogen Safety*, 2005.

[21] S. Kim, T. Jang, T. Oli and C. Park, "Behavior of Barrier Wall under Hydrogen Storage Tank Explosion with Simulation and TNT Equivalent Weight Method," *Applied Sciences,* Vols. 13, no. 6, March 2023.

[22] M. Liu and e. al., "The Effect of Explosions on the Protective Wall of a Containerized Hydrogen Fuel Cell System," *Energies,* Vols. 16, no. 11, June 2023.

[23] I. Sochet, S. Eveillard, J. Vincont, P. Piserchia and X. Rocourt, "Influence of the Geometry of Protective Barriers on the Propagation of Shock Waves," *Shock Waves,* vol. 27, pp. 209-219, April 2016.

[24] O. Alshammari, O. Isaac, D. Clarke and S. Rigby, "Mitigation of Blast Loading through Blast-obstacle Interaction," *International Journal of Protective Structures,* Vols. 14, no. 3, pp. 357-389, September 2022.

[25] T. Schunck and D. Eckenfels, "Blast Mitigation by Perforated Plates using an Explosive Driven Shock Tube: Study of Geometry Effects and Plate Numbers," *Applied Sciences,* Vols. 3, no. 731, June 2021.

[26] A. Britan, A. Karpov, E. Vasilev, O. Igra, G. Ben-Dor and E. Shapiro, "Experimental and Numerical Study of Shock Waver Interaction with Perforated Plates," *Journal of FLuids Engineering,* vol. 126, pp. 399-409, May 2004.

[27] A. Britan, O. Igra, G. Ben-Dor and H. Shapiro, "Shock Wave Attenuation by Grids and Orifice Plates," *Shock Waves,* Vols. 2006, no. 16, pp. 1-15.

[28] G. Langdon, I. Rossiter, V. Balden and G. Nurick, "Performance of Mild Steel Perforated Plates as a Blast Wave Mitigation Technique: Experimental and Numerical Investigation," *International Journal of Impact Engineering,* vol. 37, pp. 1021-1036, June 2010.

[29] T. Schunck, M. Bastide, D. Eckenfels and J. Legendre, "Explosion Mitigation by Metal Grid with Water Curtain," *Shock Waves,* vol. 31, pp. 511-523, May 2021.

[30] O. Ram, G. Ben-Dor and O. Sadot, "On the Pressure Buildup behind an Array of Perforated Plates Impinged by a Normal Shock Wave," *Experimental Thermal and Fluid Science,* vol. 92, pp. 211-221, November 2017.

[31] W. Xiao, M. Andrae and N. Gebbeken, "Experimental Investigations of Shock Wave Attenuation Performance using Protective Barriers Made of Woven Wire Mesh," *International Journal of Impact Engineering,* vol. 131, pp. 209-221, May 2019.

[32] L. Chen, L. Zhang, Q. Fang and Y. Mao, "Performance Based Investigation on the Construction of Anti-blast Water Wall," *International Journal of Impact Engineering,* vol. 81, pp. 17-33, March 2015.

[33] A. Britan, G. Ben-Dor, O. Igra and H. Shapiro, "Shock Waves Attenuation by Granular Filters," *International Journal of Multiphase Flow,* vol. 27, pp. 617-634, July 2000.

[34] G. Ben-Dor, A. Britan, T. Elperin, O. Igra and J. Jiang, "Experimental Investigation of the Interaction Between Weak Shock Waves and Granular Layers," *Experiments in Fluids,* vol. 22, pp. 432-443, September 1996.

[35] H. Ousji and e. al., "Air-blast Response of Sacrificial Cladding Using Low Density Foams: Experimental and Analytical Approach," *International Journal of Mechanical Sciences,* Vols. 128-129, pp. 459-474, May 2017.

[36] L. Blanc, A. Jung, S. Diebels, A. Kleine and M. Sturtzer, "Blast Wave Mitigation with Galvanised Polyurethane Foam in a Sandwich Cladding," *Shock Waves,* vol. 31, pp. 525-540, October 2021.

[37] E. Badshah, A. Naseer, M. Ashraf, F. Shah and K. Akhtar, "Review of Blast Loading Models, Masonry Response and Mitigation," *Shock and Vibration,* 2017.

[38] S. Sastry, P. Budarapu, Y. Krishna and S. Devaraj, "Studies on Ballistic Impact of the Composite Panels," *Theoretical and Applied Fracture Mechanics,* vol. 72, pp. 2-12, July 2014.

[39] Viracon, "Laminated Glass for Blast Mitigation," October 27, 2004.

[40] Y. Chen, W. Huang and S. Constantini, "Blast Shock Wave Mitigation using the Hydraulic Energy Redirection and Release Technology," *PLos One,* Vols. 7, no. 6, p. e39353, June 2012.

[41] Western Washington University, "PPE Hazard Assessment," *Environmental Health and Safety.*

[42] D. M. Brooks and A. M. Glover, "Comparison of Side-on Peak Overpressure Predictions and Measurements for Type IV Composite Overwrapped Pressure Vessel Catastrphic Failure," Sandia National Laboratories, SAND2022-10372, Albuquerque, New Mexico, 2022.

[43] Center for Chemical Process Safety, "Chapter 6: Vapor Cloud Explosions," in *Guidelines for Vapor Cloud Explosion, Pressure Vessel Burst, BLEVE and Flash Fire Hazards*, Wiley, 2010, pp. 168-174.

[44] H. L. Brode, "Blast Wave from a Spherical Charge," *The Physics of Fluids,* vol. 2, no. 2, pp. 217-229, 1959.

[45] Center for Chemical Process Safety, "Chapter 7: Pressure Vessel Bursts," in *Guidelines for Vapor Cloud Explosion, Pressure Vessel Burst, BLEVE and Flash Fire Hazards*, Wiley, 2010, pp. 260-279.

[46] B. Hemmatian, E. Planas and J. Casal, "Comparative analysis of BLEVE mechanical energy and overpressure modelling," *Process Safety and Environmental Protection,* pp. 138-149, 2017.

[47] A. Rhatgi, "WebPlotDigitizer, Version 5," May 2024. [Online]. Available: https://automeris.io/posts/.

[48] The Mathworks, Inc., *MATLAB (2023a),* 2023.

[49] J. Geng, Q. Baker and K. Thomas, "Pressure Vessel Burst Directional Effects," in *Proceedings of the ASME 2011 Pressure Vessels & Piping Conference PVP2011*, Baltimore, Maryland, 2011.

[50] B. Ehrhart and E. Hecht, "SAND2022-16425, Hydrogen Plus Other Alternative Fuels Risk Assessment Models (HyRAM+) Version 5.0 Technical Reference Manual," November 2022.

[51] Nuclear Regulatory Commission, "Regulatory Guide 1.91, Evaluations of Explosions Postulated to Occur at Nearby Facilities and on Transportation Routes Near Nuclear Power Plants," April 2013.

[52] R. Christian, C. Otani, K. Vedros and A. Glover, "Preliminary Risk Analysis of Nuclear Co-located Hydrogen and Syngas Production".

[53] IEP Technologies, "Explosion Protection Systems," [Online]. [Accessed 12 April 2024].

DISTRIBUTION

Email—Internal

Name	Org.	Sandia Email Address
Austin Glover	8854	amglove@sandia.gov
Chris LaFleur	8854	aclafle@sandia.gov
Melissa Louie	8854	mlouie@sandia.gov
Dusty Brooks	8854	dbrooks@sandia.gov
Technical Library	1911	sanddocs@sandia.gov

Sandia National Laboratories

Sandia National Laboratories is a multimission laboratory managed and operated by National Technology & Engineering Solutions of Sandia LLC, a wholly owned subsidiary of Honeywell International Inc. for the U.S. Department of Energy's National Nuclear Security Administration under contract DE-NA0003525.